IN VITRO SELECTION OF ANTI-GLIADIN SINGLE-DOMAIN ANTIBODIES FROM A NAÏVE LIBRARY AND ITS APPLICATION FOR cDNA-DISPLAY MEDIATED IMMUNO-PCR

(ナイーブライブラリからの抗グリアジン一本鎖重鎖抗体の試験管内淘汰とそのcDNAディスプレイ-イムノPCR法への応用)

By

RANWADANA MUDIYANSELA GEDARA CHATHUNI SAMANTHIKA KUMARI JAYATHILAKE

17DS055

A dissertation submitted as a partial fulfilment of the requirement for the Degree of Doctor of Philosophy in Science and Engineering

Supervisor: Professor Naoto Nemoto

Department of Functional Material Science

Graduate School of Science and Engineering

Saitama University

March 2020

Dedicated to the posterity of students

Abstract

Gluten intolerance, or adverse intestinal reactions to gluten, is a fairly common problem among certain groups of people. Celiac disease is the most severe form of gluten intolerance, which can lead to permanent damage in the digestive system. Since lifelong avoidance of gluten is the only available treatment, development of reliable techniques to identify gluten contamination in food is important. Gliadin, a component of gluten, is known to play a major role in gluten toxicity. The cDNA display method is used in this study which is a promising in vitro display technique, which uniquely converts an unstable mRNA-protein fusion molecule to a stable mRNA/cDNA-protein fusion molecule using a well-designed puromycin linker. This study was aimed to select specific single-domain antibodies against toxic gliadin from an alpaca-derived naïve VHH library using cDNA display method and to apply newly developed cDNA display mediated immuno-PCR (cD-iPCR) method in determining the affinity of selected VHHs against gliadin and finally to compare the results of cD-iPCR with other affinity assays (Pull-down assay and ELISA). Three candidate VHHs were successfully selected and the affinities of the VHHs were observed by pulldown assay and indirect ELISA method. Those affinity results were in line with the novel cD-iPCR assay results indicating the accurate applicability of the method. In addition, cD-iPCR method was successfully applied to detect gliadin in actual food samples. VHH1 and VHH2 were the best binders toward gliadin compared with VHH3 in all assays performed, including the cD-iPCR assay. We believe this work demonstrates the potential application of the cDNA display method in selecting binders against toxic and heterogeneous targets such as gliadin with an immunization-free preparation manner.

Table of contents

List of figures

List of tables

Chapter 1

Introduction and Literature review

1. 1. Introduction

The prevalence of wheat/gluten toxicity, along with adherence to a strict gluten-free diet, is becoming a serious dietary concern worldwide (Ontiveros *et al.*, 2018; Inna Spector Cohen *et al*, 2019; Yano, 2019). Celiac disease (CD) has become one of the most common autoimmune diseases, resulting in lifelong intolerance to gluten in sensitized individuals (Balakireva *et al.*, 2016; Lionetti *et al.*, 2019). CD induces a T cell-mediated inflammatory process in the small intestine, which leads to an enteropathy with impairment of the mucosal surface and, consequently, substandard absorption of nutrients (Chu and Wen, 2013). The unique composition of cereal prolamins in wheat, barley and rye renders them resistant to human gastrointestinal proteolytic enzymes. This is due mainly to their unusually high content of glutamine and proline residues, which leads to incomplete degradation of these proteins during normal human digestion (Shan *et al.*, 2002). Such partial degradation is nowadays thought to be the key element in the activation of the immune response in the small-bowel mucosa and the progression of celiac disease in genetically susceptible individuals. Celiac disease is an autoimmune-mediated disorder of the small-intestine characterized by gluten-dependent, gradually developing villous atrophy and crypt hyperplasia together with local inflammation in the small-bowel mucosa. In addition, the presence of circulating and small-bowel mucosal autoantibodies is markedly related to the disease. The lifetime disease can be treated only by strict exclusion of the cereal prolamins (gliadin, hordein and secalin), termed gluten, in the context of celiac disease (Fasano and Catassi, 2001; Parzanese *et al.*, 2017; Husby, Murray and Katzka, 2019; Saeed, Assiri and Cheema, 2019**).** The main storage

proteins of wheat, barley and rye are called gluten. Gluten is a mixture of proteins, called prolamins and glutelins. The function of storage proteins is to store nitrogen, carbon and sulphur in the grain endosperm. Prolamins of wheat have the special characteristic of forming viscoelastic dough, which is important in wheat baking, whereas prolamins of other cereal species lack this property. Unfortunately, these same proteins are also harmful for gluten-sensitive people, e.g. for people with celiac disease. In the context of celiac disease, prolamins of wheat, barley and rye are often called gluten, and hence the term gluten-free is generally used. Prolamins in wheat are called gliadins. It is the alcohol-soluble fraction of gluten, commonly considered to be toxic for some people (Scherf, Koehler and Wieser, 2016; Urade, Sato and Sugiyama, 2018). Furthermore, gliadins can be subdivided into categories, according to the amino acid composition and molecular weight, i.e., α/β, and γ gliadins (Geisslitz *et al.*, 2018; Lim *et al.*, 2018; Manai *et al.*, 2018). People with gluten-related disorders must remove gluten from their diet strictly, because there are no reliable medical treatments for food allergies to date. Hence, the assurance of the absence of gluten in food is of paramount importance.

Recently, considerable attention has been devoted to the immunodetection technologies using single variable domain from a heavy chain antibodies (VHH) (Hamers-Casterman *et al.*, 1993; Salvador, Vilaplana and Marco, 2019). VHH antibodies are the antigen-binding fragments of heavy chain only antibodies (HcAb), which are naturally produced in camelids (Wesolowski *et al.*, 2009). VHH antibodies are approximately 10-fold smaller than conventional antibodies (~ 15 versus ~ 150 kDa) and the most important loop of the antigen recognition site (i.e., the CDR3 loop) is often longer than that of a VH from conventional antibodies (De Vlieger *et al.*, 2018). These antibodies exhibit several advantageous features, including high stability, versatility, specific refolding capacity, reduced aggregation tendency, and high affinity with their cognate antigens

(Hamers-Casterman *et al.*, 1993; Gonzalez-Sapienza, Rossotti and Tabares-da Rosa, 2017; De Vlieger *et al.*, 2018). Hence, VHH antibodies surpass many of the conventional antibodies in clinical therapeutics and immunodiagnostics (Eden *et al.*, 2017). Most of the practically used VHHs have been retrieved from VHH repertoires of immunized camels or llamas. However, several artificial and naïve VHH libraries also have been developed and screened recently (Sabir *et al.*, 2014; Moutel *et al.*, 2016). Naïve libraries are derived from the primary B-cells of non-immunized donors, which gives a high diversity to the library (Olichon and de Marco, 2012). Compared with synthetic or immunized libraries, naïve libraries, because of their diversity and heterogeneity, allow the identification of binding agents for any potential antigen, including toxins.

Functional approaches, such as in vitro selection, currently provide the best means available for isolating peptides and proteins with desired chemical or biochemical properties. Over the last decade, display technologies have been essential tools in the discovery of peptide and protein ligands and in delineating in vivo interaction partners. The phage (Smith and Petrenko, 1997) and ribosome display systems (Hanes and Pluckthun, 1997) have been principally used for discovery of antibodies, while the yeast two-hybrid method (Fields and Song, 1989) has been used for in vivo interaction analysis. Despite their power, technologies that require in vivo step, such as phage display and the yeast two-hybrid system face certain limitations. In phage display, libraries must be transformed into bacteria, limiting the number of possible independent sequences to 10^9–10^{10}. The total number of sequences represented can be further decreased by other issues including degradation of unfolded molecules, poor expression in the bacterial host, failure in processing to the phage surface, failure to fold in the oxidizing periplasmic space of *Escherichia Coli*, or toxicity of the gene product. Similarly, the two-hybrid system requires that the interaction partners be cloned into yeast, limiting the number of constructs examined to 10^6-10^7.

The cDNA display peptide and protein selection system provides an alternative method that can be applied to both ligand discovery and interaction analysis problems (Yamaguchi *et al.*, 2009; Ueno and Nemoto, 2012). In this approach, encoded peptide and protein libraries are covalently fused to their own cDNA. Fusion synthesis is possible because the message can act as both template for cDNA and peptide acceptor since it contains a 3'-puromycin molecule. Puromycin serves as a chemically stable, small molecule mimic of aminoacyl tRNA. Routinely 10–40% of the input mRNA template can be converted to fusion product, resulting in more than 5 x 10^{13} mRNA-protein fusions per milliliter of translation reaction. Overall, the cDNA display system allows libraries with sequence complexity approximately 10,000-fold that of phage display, 10^{6}-fold over yeast display or yeast two- and three- hybrid systems, and approximately 10^{9}-fold over colony screening approaches (Arnold, 1999). In most the cDNA display experiments, polypeptides with relatively short chain lengths (10–110 amino acids) have been successfully used. Larger proteins have been studied as well (e.g. anti-GFP-VHH (Anzai *et al.*, 2019) and anti-BSA-VHH (unpublished observation), but these typically form fusion products with somewhat reduced efficiency. Even for such proteins, libraries can still be readily constructed that are orders of magnitude larger than a typical phage display library. The method proved to screen many affinity peptides/VHHs successfully without using experimental animals (Yamaguchi *et al.*, 2009; Suzuki *et al.*, 2018; Terai, Anzai and Nemoto, 2019). This method has several characteristics that assist in remediating many drawbacks (e.g. instability, limited diversity or small library size, cell toxicity of proteins, effect of fused coat proteins, and difficult handling) that are occurring either cell dependent (i.e., phage display, bacterial display, yeast display) or cell-independent (i.e., ribosome display, mRNA display) *in vitro* selection. (Ueno and Nemoto, 2012; Nemoto *et al.*, 2014; Tanemura *et al.*, 2015). The key feature of the cDNA display method is the easy to use preparation

using a unique puromycin linker, which is hybridized and photo-ligated to the 3'-end of mRNA. Linker contains five functional features: a photo cross-linking site to ligate with mRNA by cnvK, a puromycin moiety for the covalent linking of the synthesized protein, and a biotin moiety for immobilization onto SA beads for purification and reverse transcription, a priming site for reverse transcription to synthesize cDNA and a restriction site for release from SA beads with RNase. In addition, the linker has FITC moiety for detection (Yamaguchi *et al.*, 2009; Mochizuki *et al.*, 2011, Mochizuki *et al.*, 2015).

Taking the covalent bond formation of the protein and DNA in the cDNA display method into consideration, an immuno-PCR method called cD-iPCR has been developed (Anzai *et al.*, 2019), which was also used as a new immunodetection technique in the present study. Immuno-PCR, often abbreviated as iPCR, is an extremely powerful method in detection and quantification of low abundance biomarkers that exist in biological samples (e.g., serum and urine). It acts as a bridge between immuno-reaction and signal amplification. In most cases, iPCR relies on the use of a detection antibody which has been conjugated to a reporter oligonucleotide, followed by the quantification of the analytes using real-time PCR of the reporter (Sano, Smith and Cantor, 1992). The cD-iPCR, which takes an advantage of the structural characteristics of cDNA display, proved to work in detection of target proteins both in direct and sandwich-type formats (Anzai *et al.*, 2019). The cD-iPCR method offers several merits over the conventional iPCR and PD-iPCR, which include 1) based on a covalent homogeneous DNA-antibody conjugation, 2) non-viral, and 3) almost a ready to use reagent, 4) easy to perform by biologists without expertise in organic chemistry. Concisely, current study was approached to explore specific VHH antibodies against whole gliadin from an alpaca-derived naïve VHH library, using the cDNA display method as a powerful cell-free display tool.

1.2. Gliadin Intolerance and celiac disease

1.2.1. Wheat Storage Proteins

Bread wheat (*Triticum aestivum* L.) is one of the most important food crops, with current annual global production of over 680 million tons providing approximately one-fifth of the total calorific input of the world population (Rasheed *et al.*, 2014). Wheat proteins can be classified according to their solubility in different solvents (Osborne, 1907). The groups of protein in wheat are the albumins soluble in water, the globulins soluble in salt solutions, alcohol-soluble prolamins known as the prolamins and glutenins. The prolamin proteins can be further divided into subunits of high molecular weight (HMW) and low molecular weight (LMW). These subunits form polymers, linked by disulphide bonds and responsible for the baking quality of wheat flour in forming cohesive, elastic dough when mixed with water (Shewry *et al.*, 2000). Gliadins are monomeric and can be separated into α/ β-, γ- and ω-gliadins based on their amino acid composition.

Table 1.1. Prolamins of wheat, barley, rye and oats. The one letter code for amino acid is used in the repetitive domain. F-Phenylalanine, G-Glycine, H-Histidine, I-Isoleucine, L-Leucine, P-Proline, Q-Glutamine, S-Serine, T-Threonine, V-Valine, Y-Tyrosine.

Cereal	Prolamin subgroup	MW (kDa)	%	Repetitive domain
Wheat	α/β-Gliadins	28-35	28-33	PQPQPFP and PQQPY (50%)
	γ-Gliadins	31-35	23-31	PQQPFPQ (40%)
	$\omega_{1,2}$-Gliadins	39-44	4-7	PQQPFPQQ (90%)
	ω_5-Gliadins	49-55	3-6	QQQ-F/I/L-P
	LMW	32-39	19-25	PQQPPPFS and QQQQPVL (26%)
	HMW subunit x	83-88	4-9	PGQGQQ.GYYPTS-P/L-QQ and GQQ

	HMW subunit y	67-74	3-4	PGQGQQ and GYYPTS-P/L-QQ
Barley	B-Hordeins	36-44	70-80	PQQP (<30%)
	C-Hordeins	55-70	10-20	PQQPFPQQ
	D-Hordeins	90-110	<10	P-G/H-QGQQ.GYYPSXTSPQQ
	γ-Hordeins	36-44	<10	PQQPFPQ
Rye	ω-Secalins	48-53	17	PQQPFPQQ
	γ-40 Secalins	36-44	24	QPQQPFP
	γ-75 Secalins	70	46	QQPPQQPFP
	HMW	~100	7	QQPGQG
Oats	α-Avenins	12-18	Minor	PFVQQQ
	β-Avenins	22-35	Minor	

Data collected from Shewry, 1999; Shewry and Tatham, 1990; Shewry and Tatham, 1997; Shewry *et al.*, 1995; Shewry *et al*., 1996; Shewry and Tatham, 1999.

1.2.2. Gliadins

Monomeric wheat prolamins or gliadins, are divided into subgroups as α-, γ-, β- and ω-gliadins. The group of α- gliadins is generally the major group, comprising between 44 and 60% of the total gliadin content. The second largest group is γ- gliadins (31–46%), and together these groups account for about 80% of wheat gliadins (Shewry and Tatham 1990). The α- and γ- gliadins are often combined and simply referred to as α- gliadins because of the high similarity of their N-terminal amino acid sequences. The sizes of α- and γ- gliadins are approximately 36 000–44 000 g/mol, they contain about 250–300 amino acid residues and are rich in sulphur. The α-gliadins are typical for wheat and they are thought to be the most harmful fraction for people with celiac disease. Although rye and barley are considered as harmful for celiacs as wheat, they do not contain

similar proteins (Shewry and Tatham 1990). The α-gliadins contain long repeats of glutamine residues along with typical repetitive domains. The γ- gliadins are also repetitive and mostly monomers; however, polymeric forms also exist (Shewry and Tatham 1990). The rest of the gliadins, about 10–20%, are sulphur-poor ω-gliadins. Their sizes are between 44 000–78 000 g/mol. Due to the highly repetitive nature of ω-gliadins, about 80% of their amino acid content is glutamine, glutamic acid, proline and phenylalanine residues (Table 1.1). Since ω-gliadins are poor in sulphur they do not contain disulphide bonds in their structure, they retain their solubility after heat treatment. Their solubility was reported to remain the same in processed samples as the solubility of sulphur-containing α- and γ- gliadins decreased considerably (Skerritt and Smith 1985). Immediate allergic reactions have been associated with α- and γ- gliadins (Palosuo *et al*., 2001).

1.2.3. Gluten Intolerance

Gluten intolerance is an umbrella term integrating three major types of gluten-related disorders: autoimmune celiac disease (CD), allergy to wheat and non-celiac gluten sensitivity (NCGS). Although these disorders possess similar symptoms, which include bloating, vomiting and diarrhea, a number of principle differences of their pathogenesis are remarkable (Balakireva, 2016). Celiac disease (CD) is a serious autoimmune disease that occurs in genetically predisposed people where the ingestion of gluten leads to damage in the small intestine. The reaction to gluten causes villous atrophy or flattening of the cells lining the small intestine, which can lead to malabsorption of nutrients with wide-reaching symptoms. Classical celiac disease, patients have signs and symptoms of malabsorption, including diarrhea, steatorrhea (pale, foul-smelling, fatty stools), and weight loss or growth failure in children. Dermatitis herpetiformis is celiac disease that manifests as a skin rash. The rate of CD is higher among relatives of those who are diagnosed,

but anyone with the genetic predisposition can develop celiac disease at any age. First-degree relatives whether or not experiencing symptoms, should always be screened, since there is a 1 in 10 risk of developing celiac disease. Second-degree relatives and families with multiple individuals with celiac disease also have an increased risk of developing the disease (Al-Toma *et al.*, 2019). Currently it is estimated that about 1% of the population has celiac disease, although 83% of those people are still undiagnosed. While research continues to work towards pharmaceutical or other treatments, at this time the only treatment for celiac disease is to maintain a gluten-free diet for life (Anania *et al.*, 2017; Inna Spector Cohen *et al.*, 2019; Husby, Murray and Katzka, 2019; Lionetti *et al.*, 2019; Saeed, Assiri and Cheema, 2019). Non-Celiac Gluten Sensitivity (NCGS) is a syndrome characterized by intestinal and extra-intestinal symptoms related to the ingestion of gluten-containing food, in subjects that are not affected by either celiac disease or wheat allergy (Catassi *et al.*, 2015). It is not an immunoglobulin E (IgE) (as with wheat allergy) nor autoimmune reaction (as with CD). Most of the analyzed studiers agree that NCGS would need to be diagnosed only after exclusion of celiac disease and wheat allergy, and that a reliable serological marker is not available presently. The mechanisms causing symptoms in NCGS after gluten ingestion are largely unknown, but recent advances have begun to offer novel insights. The estimated prevalence of NCGS, at present, varies between 0.6 and 6% (Casella *et al*., 2018). Reactions can begin up to 48 hours after ingesting gluten and last for much longer. To diagnose GS, it is first necessary to rule out CD, wheat allergy or other possible causes of symptoms. Then, if improvement is seen when following a gluten-free diet, gluten sensitivity may be diagnosed. Life-long adherence to a gluten-free diet is the only treatment for GS at this time (Catassi *et al.*, 2015, Biesiekierski, 2013, Carroccio *et al.*, 2012). Wheat allergy is an immune reaction to any of the hundreds of proteins in wheat. It is not the same as Celiac Disease, in which a person needs to

follow a gluten free diet. Someone with a wheat allergy will have an instant reaction to eating wheat. When a person has a wheat allergy, one type of white blood cells, called T-cells, send out immunoglobulin E (IgE) antibodies to "attack" the wheat. At the same time, local tissues in the body send out natural chemical messengers to alert the rest of the body that there is a problem. This reaction happens very fast (within minutes to a few hours) and can involve a range of symptoms from nausea, abdominal pain, itching, swelling of the lips and tongue, to trouble breathing, or anaphylaxis (a life-threatening reaction). A person with a wheat allergy must avoid eating any form of wheat but does not have trouble tolerating gluten from non-wheat sources. (It is possible for a person to be both allergic to wheat and have CD or GS.) Children who are allergic to wheat may out-grow the allergy, but adults with an allergy to wheat usually have it for life. The only treatment is a wheat-free diet (Czaja-Bulsa and Bulsa, 2017, Sapone *et al.*, 2012, Longo *et al.*, 2013).

1.2.4. Autoimmune enteropathy of celiac disease

Celiac disease is induced by gluten-containing food in people carrying HLA-DQ2 or DQ8 haplotype (human leukocyte antigen Class II with DQ2 and/or DQ8 molecules on antigen-presenting cells). In the small intestinal mucosa CD4+ T-cells are stimulated by gliadin peptides only when presented by DQ2 or DQ8 MHC (The major histocompatibility complex) molecules on the surface of antigen-presenting cells. This binding triggers proliferation of pathogenic gluten-specific T-cells (Barton and Murray, 2008). After gluten enters into the digestive system, glutamine and proline-rich gluten composing proteins are partially hydrolyzed by proteases presented in the gastrointestinal tract. The upregulation of intestinal peptide zonulin, involved in tight junction regulation, appears to be partly responsible for the increased permeability characteristic of the gut (Figure 1.1). As a result, generated gluten-derived peptides reach the

lamina propria (mucosa) by transcellular or paracellular transport where they are modified by tissue transglutaminase (tTG) enhancing their affinity to MHC II molecules, and thereby making them toxic and immunogenic in HLA-DQ2 or DQ8 containing patients (Van Heel and West, 2006, Wang *et al.*, 2000, Schuppan, 2000). The repetitive presence of glutamine and proline residues determines the gluten-derived peptides as a preferred substrate for tTG. tTG-mediated modifications occur in two ways: deamidation (cleavage of the ε-amino group of a glutamine side chain) or more frequently transamidation (cross-linking of a glutamine residue from the gliadin peptide to a lysine residue of tTG). Further peptides presentation by HLA-DQ2/DQ8 protein subunits in the surface of dendritic cells to gluten-specific T cells induces two levels of immune response: the innate response and the adaptive (T-helper cell mediated) response with the production of interferon-γ and IL-15. As a result, it causes immune-mediated enteropathy, intestinal inflammation, followed by the atrophy of villi, crypt hyperplasia and increased infiltration by intraepithelial lymphocytes. It also produces weight loss and chronic diarrhea. Although the causative agent is a dietary protein, the disease has marked autoimmune features, which are indicated by the presence of autoantibodies against tTG. Cross-linking between gliadin and tTG is covalent resulting in the formation of new epitopes, which trigger the primary immune response, and by which the autoantibodies against tTG are developed (Nilsen *et al.*, 1998, Dewar *et al.*, 2004). CD is not only characterized by gastrointestinal symptoms but also by extraintestinal manifestations, some of which are a direct consequence of autoimmunity responses; for example, dermatitis herpetiformis or gluten ataxia while others are an indirect consequence of anaemia, such as osteoporosis, short stature and delayed puberty (Husby *et al.*, 2012, Fasano and Catassi, 2012, Leffler *et al.*, 2015).

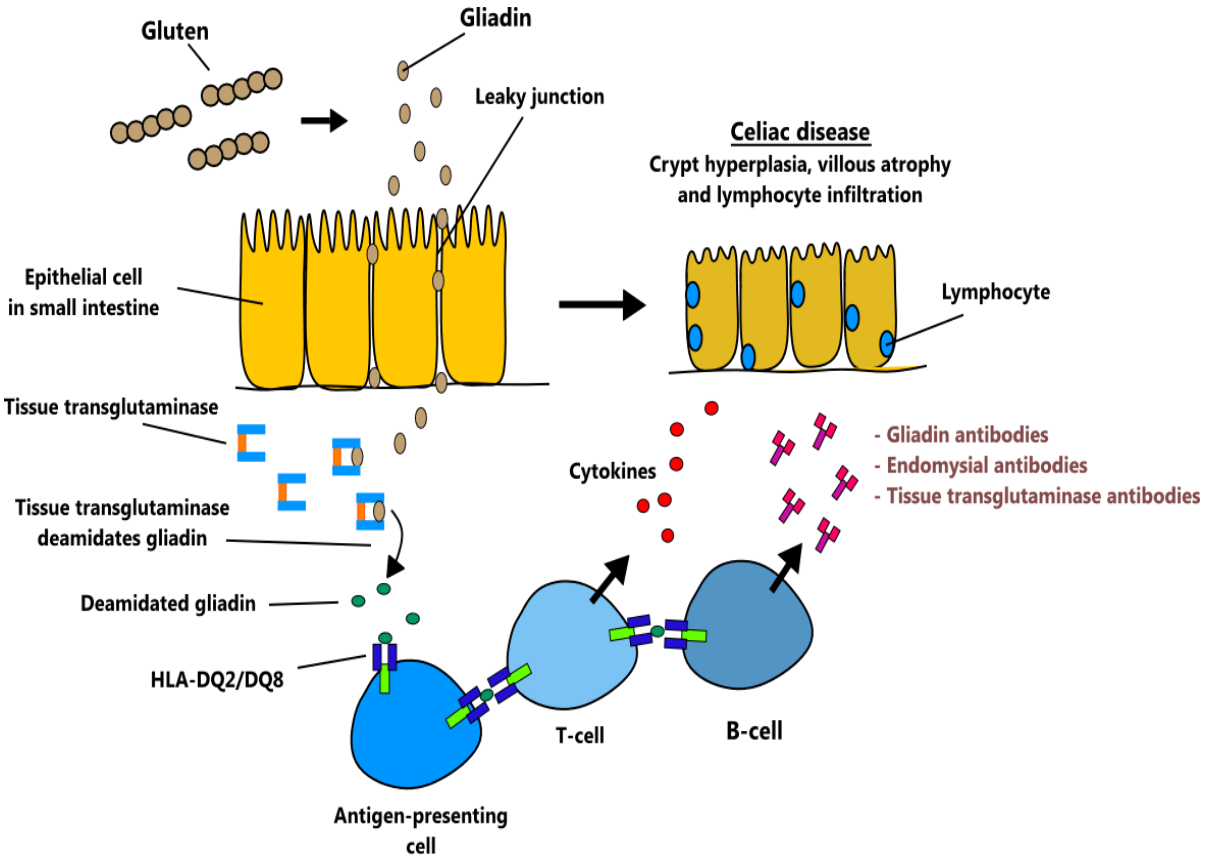

Figure 1.1. Schematic representation of major pathways in celiac disease (CD) pathogenesis. Once gliadin reaches the lamina propria, it is deamidated by tissue transglutaminase (tTG). Deamidated gliadin then reacts with antigen-presenting immune cells of the HLA-DQ2 or HLA-DQ8 subtype. Antigen-presenting cells stimulate T-cell and B-cell responses that promote cytokine release, antibody production, and lymphocyte infiltration. These inflammatory processes lead to villous atrophy and crypt hyperplasia in epithelial cells. (Green and Cellier, 2007).

1.3. Camelid single domain antibodies (VHH)

VHH domains derived from heavy-chain antibodies of camelids, commonly named nanobodies, are single-domain antigen-binding fragments with a large potential for numerous applications in research, biotechnology and medicine. Lineage specific gene duplications and mutations account for the distinct IgG subclasses found in llamas and other camelids (camel, dromedary, vicuña,

guanaco). Peculiar to camelids is the complete lack of light chains and of the CH1 domain by antibodies of the IgG2 and IgG3 subclasses (Hamers-Casterman *et al.,* 1993; Nguyen *et al.,* 2002) while camelid IgG1 antibodies display a conventional anibody structure. IgG1 comprises up to 75% of of llama serum IgGs with IgG2 and IgG3 making up a combined 25% – 45%. The variable domain of the so-called heavy chain only antibodies (hcAb) is linked directly to the CH2 domain by the hinge region. Llama IgG2 and IgG3 subclasses differ in the length of the hinge regions. IgG2 is a long hinge hcAb whereas IgG3 comprises the short hinge subtype. Distinct from the antigen binding paratope of conventional antibodies which is determined by combined variable regions of both light and heavy chains, a single variable domain of the hcAb is responsible for antigen binding. The domain is designated VHH (variable domain of the heavy chain only antibody) to distinguish it from the VH counterpart of conventional antibodies. They exhibit several superior properties compared to conventional antibody scaffolds, such as enhanced solubility, high immunogenicity and the unique ability to bind cryptic epitopes; due to their small size and a third complementarity determining region (CDR3) of unusual length. VHHs can be cloned and recombinantly expressed as the smallest antibody fragment with antigen binding properties (Muyldermans *et al.*, 2001). Due to their small size, these single domain antibodies are also referred to as Nanobodies® (Nbs). Evolutionary substitution of four hydrophobic amino acids at the former interface to the VL domain to hydrophilic residues accounts for the high solubility and stability of VHH domains. This permits the recombinant expression of VHHs as water soluble protein molecules (Vu *et al.*, 1997). VHHs are easily expressed in *E.coli* as periplasmic proteins or in eukaryotic cells as secretory proteins with high yields at relatively low costs (Wesolowski *et al.*, 2009; Holliger and Hudson, 2005). They are thermostable and are able to withstand harsh pH conditions. Furthermore, VHHs show superior tissue penetration and quick systemic clearance

compared to conventional antibodies. VHHs are versatile, easily reformatted when required, into homo– or hetero–polymeric molecules to increase avidity; into bi-parotopic formats for specific tissue targeting or to increase serum half-life; or into VHH-Fc fusion proteins to reconstitute effector functions or facilitate in vivo recycling and increase serum half-life (Scheuplein *et al.*, 2010; Tijink *et al.*, 2008). Importantly, the CDR3 regions of VHH are on average longer than in classical antibodies reaching as long as 26 amino acids (Desmyter *et al.*, 1996). These long CDR3 regions can form finger-like structures that reach into crevices on protein surfaces inaccessible to flat paratopes of conventional antibodies. Indeed, following immunization of llamas with enzymes carrying a deep active site crevice, the induced heavy chain antibodies often show a propensity to block the enzymatic activity (Desmyter *et al.*, 1996; Koch-Nolte *et al.*, 2007). Schematic representation of the structure of a conventional IgG and the variable heavy-chain antibody fragment (VHH) is shown in figure 1.2.

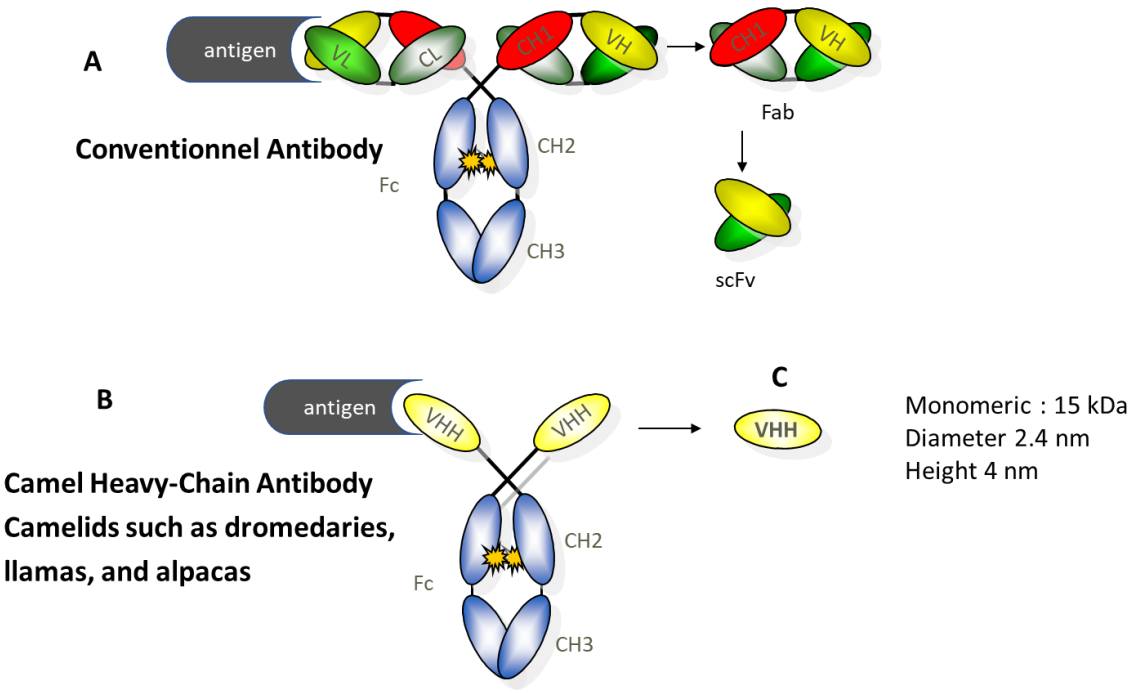

Figure 1.2. Schematic representation of the structure of Antibodies. (a conventional IgG, a heavy-chain IgG antibody and the variable heavy-chain antibody fragment (VHH) that can be generated of the latter). A) A conventional IgG antibody is a dimeric molecule, and each monomer comprises a heavy chain and a light chain. The heavy chain consists of the constant domains (CH1, CH2 and CH3) and the variable domain (VH). The light chain has only one conserved domain (CL) and a variable domain (VL). B) Heavy-chain antibodies found in llama and camel are only composed of heavy-chains and lack the light chain completely, as shown in this Figure. The antigen-binding domain consists of only the VH domain, which is referred to as VHH (variable heavy-chain antibody fragment), to distinguish it from a normal VH. C) The VHH can be expressed as a prolate-shaped, soluble molecule of ~15 kDa. known as VHH or Nanobody.

1.4. The principal of evolutionary molecular engineering

1.4.1. Evolutionary molecular engineering

The principle of molecular evolution served as the key mechanism for in vitro selection, where genotype is represented by a sequence that can be amplified (which in most cases means being copied by polymerase), and phenotype is represented by the functional trials of the molecule, i.e. binding aptamer (Gold *et al.*, 1993). Similar to natural selection, the process starts with a large pool of random molecules, which in most cases are nucleic acids or polypeptides, and certain selection pressure would be applied to the random pool or an aptamer library. Those molecules that survive from the selection pressure will be amplified. They will either become the starting point for the next round of selection or be sequenced for further analysis at the end of selection process (Figure 1.3).

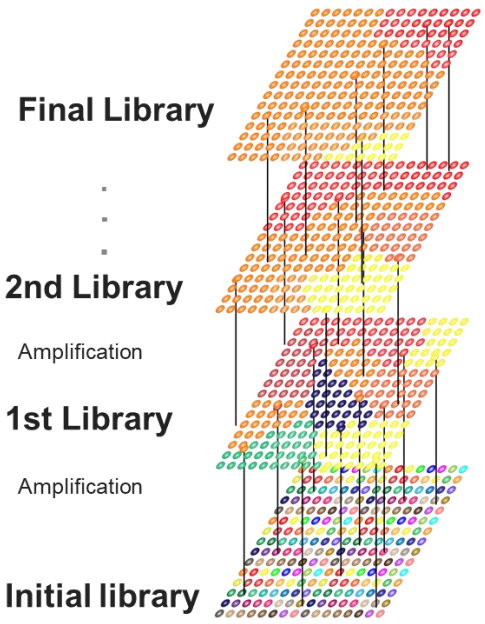

Figure 1.3. A schematic representation of the in vitro selection approach. Selection starts from construction of an initial random molecule pool or library, which precedes the selection process. After several selection rounds the enriched aptamers can be obtained.

The most important elements in the process of in vitro selection are that a pool containing enough variety of molecules; selection pressure necessary to eliminate undesired molecules; and ability to replicate selected molecules. When designing a random molecule library, several key parameters need to be considered, such as the length of the random core region, the size of the target molecule, and the degree of randomization. The diversity within the library is determined by the length of the random core region. Generally, as the length of the random region increases, the structural diversity within the library also increases. This increase in diversity allows for the presence of more complex 3D structures, which are more likely to be high-affinity moieties (Luo *et al.*, 2010). Another important parameter to consider is the size of the target molecule. The surface area available for an aptamer to interact with the target varies significantly between different classes of

molecules. An appropriate length of the random region should strike a balance between the structural diversity required for selecting high affinity aptamers and an appropriate surface coverage of the target molecule (Marshall and Ellington 2000). To select aptamers against totally new targets, a completely randomized or naive aptamer library is beneficial.

Despite the many advantages of nucleic acid aptamers, proteins still serve as the main ligand choosing by nature. One important reason is that polypeptides have much more variety in the kinds of building blocks comparing with nucleic acids, which gives the ligand more freedom in forming different kinds of bonds with the target. Besides, polypeptide does not have nuclease cleavage issue, especially for applications in vivo, and the variety charge on the surface rather than highly negatively charge would make it easier to cross biological membrane if other factors are not taken into consideration. However, the most important issue in evolution of polypeptides is how to connect the phenotype and genotype together. In vivo strategies do so by placing the phenotype on the surface while keep the genotype inside the cell, and in vitro strategies do so by covalently or non-covalently conjugating the phenotype and genotype together (Ullman, Frigotto and Cooley, 2011). There are also other selection strategies such as in vitro compartmentalization (Tawfik and Griffiths, 1998), in which a water-oil emulsion would contain both the genotype and the phenotype. Since enzymes and affinity reagents exit in nature are mostly proteins or peptides, directed evolution can be employed to improve the properties of these polypeptide molecules according to the demand of researcher.

1.4.2. In vivo selection of polypeptides by cell-dependent display methods

In vivo selection strategies include phage display (Smith and Petrenko, 1997), bacterial display (Stahl and Uhlen, 1997) and yeast display (Gai and Wittrup, 2007). Both phage display and bacterial display are first reported in 1980s, while yeast display, which involves eukaryotic cells,

is first reported in 1997. Phage display was initially designed to use phage as an expression vector, but gradually these methods developed into in vivo selection strategies. The principles for in vivo display strategies are quite similar of the in vitro selection strategies. A random DNA library, which represents the genotype, is transformed into certain type of cells, such as *E. coli* or yeast. For bacteria display and yeast display, the expressed protein, which is the phenotype, is displayed as fusion of a membrane or coat protein on the surface of the cell. For phage display, the gene encoding the protein of interest is expressed as a fusion with a coating protein and, thus, is incorporated into the outside coating of a bacteriophage, while the gene itself that expressed that protein remains encapsulated in the bacteriophage. This creates a system where every investigated protein encapsulates its genetic information. The main advantage of in vivo displays is that it provides a cellular environment to study any proteins that involved in process in living organisms, such as proteins participating in cell signaling pathways or proteins interact with cell-membrane proteins (Boder, Midelfort and Wittrup, 2000). However, there are several other disadvantages of in vivo evolution. The efficiency of transformation limits the diversity of the random library significantly. Normal library size of phage display is only 10^7 to 10^8. If a scheme calls for more diversity after each round, more cells need to be transformed and the amount labor increases enormously, which prevents the evolution through many generations.

1.4.3. In vitro selection of polypeptides by cell-independent display methods

In vitro directed evolution techniques such as ribosome display (Schaffitzel *et al.*, 1999), mRNA display (Nemoto et al, 1997) and cDNA display (Yamaguchi *et al.*, 2009) are powerful tools for protein engineering, capable of handling libraries containing up to ~10^{14} members. It normally starts with a random DNA library, which would be transcribed into message RNA (mRNA) and translated into peptide or protein. A prerequisite for the selection of proteins from libraries is the

coupling of genotype (RNA, DNA) and phenotype (protein). In ribosome display, this link is accomplished during in vitro translation by stabilizing the complex consisting of the ribosome, the mRNA and the nascent, correctly folded polypeptide. The DNA library coding for a particular library of binding proteins is genetically fused to a spacer sequence lacking a stop codon. This spacer sequence, when translated, is still attached to the peptidyl tRNA and occupies the ribosomal tunnel, and thus allows the protein of interest to protrude out of the ribosome and fold. The ribosomal complexes are allowed to bind to surface-immobilized target. Whereas non-bound complexes are washed away, mRNA of the complexes displaying a binding polypeptide can be recovered, and thus, the genetic information of the binding polypeptides is available for analysis (Zahnd *et al.*, 2007, Plückthun, 2012).

By contrast, mRNA display and cDNA display use an mRNA-DNA-puromycin fusion as its template for in vitro translation, which results in a covalent puromycin linkage between the mRNA/cDNA and the corresponding nascent peptide. This creates a highly stable selection particle, which is particularly useful for performing in vitro selections in harsh environments that are not compatible with ribosome display (Barendt *et al.*, 2013, Yamaguchi *et al.*, 2009). In comparison with in vivo evolution, in vitro selection manages to overcome most of the disadvantages mentioned above. The whole process is selection instead of screening and the diversity of library is considered by the number of necleotide or ribosome that existed in a tube, which is typically 10^{12} to 10^{13} diversity, and mutations are easily introduced through error prone PCR if necessary (Lipovsek, 2004). There are much fewer limitations to the size of desired protein reagent or the types of target. The unwanted selection pressure, which would be created by the whole process of folding, transporting, membrane insertion and complexation can be avoided with cell-free in vitro selection (Roberts, 1999).

1.4.4. cDNA Display

In cDNA display, cDNA molecule is covalently attached to the peptide or protein they encode (Figure 1.4). These cDNA-protein fusions enable in vitro selection of peptide and protein libraries of more than 10^{13} different sequences (Yamaguchi *et al.*, 2009). The cDNA display has been used to discover novel peptide and protein ligands for RNA, small molecules, and proteins, as well as to define cellular interaction partners of proteins and drugs. In addition, several unique applications are possible with cDNA display, including immuno-PCR and library construction with unnatural amino acids, and chemically modified peptides.

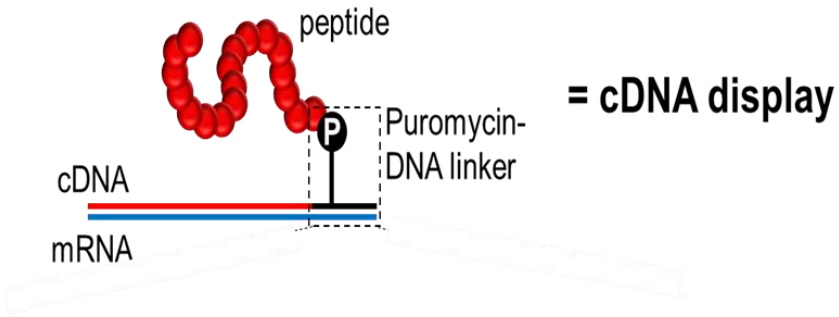

Figure 1.4. A covalent peptide-cDNA complex of cDNA display. It is conjugated via a puromycin linker. The puromycin linker makes an amide bond with the nascent peptide at its C-terminus.

The key element in mRNA display is the puromycin linker at the 3'end of mRNA Nemoto et al, 1997). Puromycin is an analogue of 3'end of a tyrosyl-tRNA. After the whole coding region is translated, the fused puromycin enters the A site of ribosome when the ribosome proceeds to form a peptide bond between puromycin and the C-terminal amino acid residue of the polypeptide chain. After cell free translation, reverse transcription is performed to generate the cDNA corresponds to the mRNA. The genotype, DNA, is thus covalently ligated with the phenotype, polypeptide. Then the genotype-phenotype fusion is incubated with the target and the binders would be recovered by elution and PCR amplified. The cDNA display has several advantages over other in vitro display

methods. The reverse transcription step before selection eliminates the possibility of selecting RNA aptamers. (Yamaguchi *et al.*, 2009; Ueno and Nemoto, 2012; Mochizuki *et al.*, 2015). Also, the puromycin linker is very small comparing (about 5KDa) with ribosome or phage, which overcomes the issue of "large display object" and the chance of causing undesirable binding is much smaller. In general, cDNA display not only possesses the advantages of in vitro selection, but also overcomes most of the "background issue" compared with ribosome display/mRNA display because of its unique a puromycin-linker DNA containing a 'ligation site', a 'biotin site' 'reverse transcription primer site' and a 'RNAs T1 cutting site' (Figure 1.5). These features facilitate extremely rapid ligation of mRNA and linker, biotin/streptavidin-based purification and cDNA synthesis by reverse transcription that together prevent degradation of mRNA, significantly reduce the execution time, allow conversion of mRNA–protein fusion (mRNA display) to cDNA–protein fusion (cDNA display), where the cDNA remains covalently linked to their encoded protein and facilitates solid-phase handling. Thus, disulfide-rich proteins can also be expressed and refolded by easy and rapid buffer exchange.

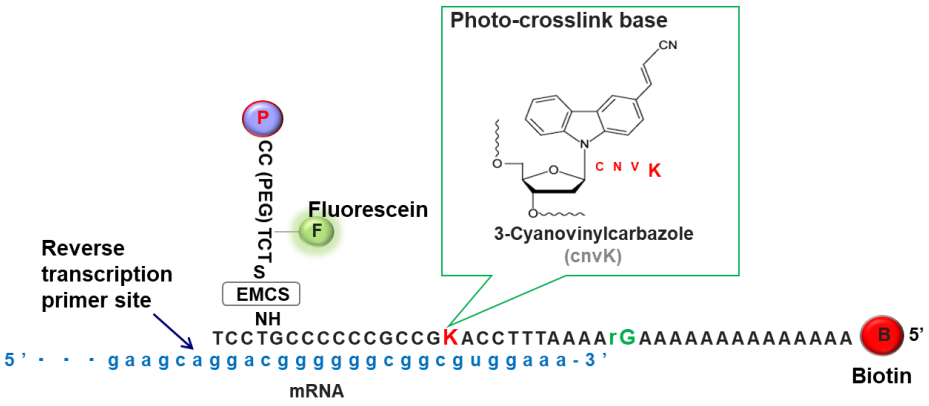

Figure 1.5. Schematic diagram of puromycin-linker DNA. Linker contains five functional features: a photo cross-linking site to ligate with mRNA by cnvK, a puromycin moiety for the covalent linking of the synthesized protein, and a biotin moiety for immobilization onto SA beads

for purification and reverse transcription, a priming site for reverse transcription to synthesize cDNA and a restriction site for release from SA beads with RNase T1. In addition, the linker has FITC moiety for detection. Specially, a UV-induced cnvK crosslinking reaction is employed to attach the puromycin linker to the 3' end of mRNA (Mochizuki et al, 2015).

1.4.5. The cDNA display mediated immune-PCR (cD-iPCR)

Detection of biomarkers that exist in biological samples (e.g., serum and urine) at low concentrations is of critical importance in basic biology and in diagnosis. Immuno-PCR (iPCR) was first described by Sano, Smith, and Cantor in 1992. The method combines the advantages of polymerase chain reaction (PCR) and immunoassay, allowing the detection of targets of interest present in a sample in extremely low concentration. The detection of specific biomarkers with high sensitivity is critical for early diagnosis and treatment. Because many key protein biomarkers are found at concentrations below the detection limits of standard enzyme linked immunoassays (ELISAs), new diagnostic tools are continuously being sought. One strategy has been to use immuno-PCR, which first requires labeling detection antibodies with synthetic oligonucleotides and utilizing polymerase chain reaction (PCR) to generate amplified signals in response to an antigen binding event. Because each antibody can be labeled with a distinct nucleic acid sequence, immuno-PCR can potentially be used for multiplexed analysis. In recent years, iPCR has been applied for detection of various antigens including cancer biomarkers (Jiang *et al.*, 2012) and viruses (Perez *et al.*, 2011).

In the development and application of iPCR, how the antibody is conjugated with reporter DNA is a critical issue. In the original iPCR method proposed by Sano *et al* a "streptavidin–protein A chimera" was used as a linker between an antibody and DNA (streptavidin bound biotinylated DNA) while protein A bound an Fc fragment of an immunoglobulin G (IgG) molecule. Such

conjugate limited the possibility to use this technique only to the direct format of target molecule detection (which is not very often used). Also, the tetrameric nature of streptavidin leads to the formation of heterogeneous DNA-antibody conjugates, which may decrease the reproducibility of iPCR. This can lead to varying, erroneous, or large background signals. Another method relies on chemical crosslinkers for directly conjugating DNA to the antibody. Although this can reduce complexity and is straightforward, conventional crosslinking chemistry reacts with the cysteine/lysine in the antibody, and the modification may compromise binding affinity of the antibody. Moreover, the number of DNA molecules bound to one antibody is heterogeneous and hard to control.

To avoid these problems, Guo *et al*. developed a new immuno-assay protocol with the aid of phage display: phage display mediated immuno-PCR (PD-iPCR) (Guo *et al*., 2006). In PD-iPCR, an engineered recombinant phage particle which expresses a single-chain antibody for the analyte is used as a ready reagent for iPCR instead of a monoclonal antibody (mAb) and chemically bound DNA. However, in PD-iPCR, the specificity of the DNA-protein linkage is compromised due to the difficulty in controlling of the number of exposed engineered coat proteins on the phage surface. Further, since these bacteriophages are genetically engineered viruses, experiments must be performed under strict legal regulations, which may be a hurdle for real-world applications.

cDNA display is one of the simplest genotype-phenotype linking methods, where cDNA is covalently fused to its coding polypeptide (which can act as the affinity probe for the target) via a uniquely designed puromycin linker (Yamaguchi *et al*., 2009; Mochizuki *et al*., 2015). The cDNA display molecules can also be regarded as antibody-DNA conjugates that are used for iPCR. The cD-iPCR system is 1) based on a homogeneous DNA-antibody conjugation, 2) non-viral, and 3) easy to perform by biologists without expertise in organic chemistry. The cDNA display molecule

is biochemically synthesized from mRNA by successive ligation with a puromycin DNA linker, in vitro translation, and reverse-transcription (Yamaguchi *et al.*, 2009). Compared with PD-iPCR, cD-iPCR has advantages such as stability under harsh conditions such as organic solvents, strong acid/base, and heat. Further, because of the conjugation mechanism using a puromycin derivative, the DNA is always conjugated to the peptide at its C-terminus with the ratio of 1:1. This method is successfully applied to the detection of a model target proteins (B domain protein A (BDA) and green fluorescent protein, GFP) and proved to work in direct- and sandwich-type detection of target proteins (Figure 1.6) (Anzai *et al.*, 2019).

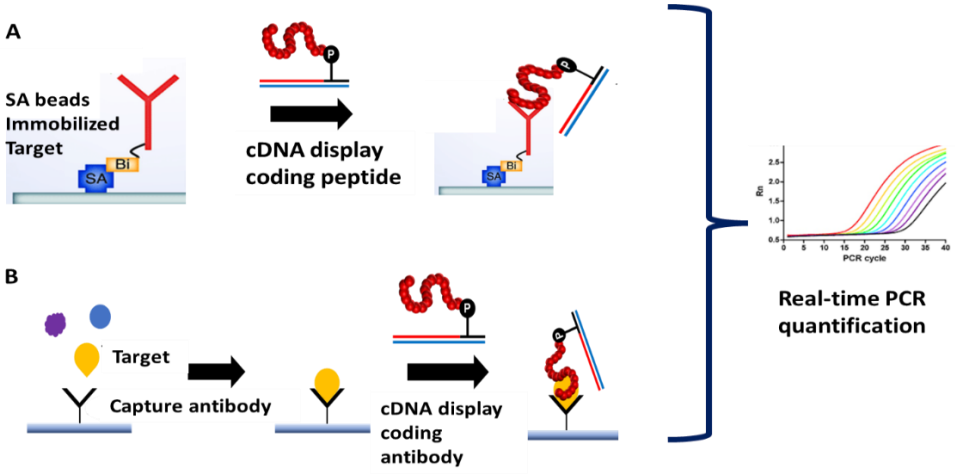

Figure 1.6. Schematic diagram of cD-iPCR for (A) direct and (B) sandwich-type detection. A target protein in a biological sample is captured on solid phase (beads or plates) using a capture beads or antibody. After washing, cDNA display of a polypeptide that has affinity to the target is added. Unreacted display molecules are washed, and resulting cDNA is quantified by qPCR. Here, cDNA display can be used both as an antibody for the target and also as a DNA marker for PCR quantification.

1.5. Research objectives

1.5.1. Main objectives

- To select specific single-domain antibodies against toxic gliadin from an alpaca-derived naïve VHH library using cDNA display method.
- To apply cDNA display mediated iPCR (cD-iPCR) to determine the affinity interactions of candidate anti-gliadin VHHs against gliadin.
- To confirm the cD-iPCR results with other affinity assays (Pull-down assay and ELISA) to determine the accuracy of cD-iPCR method.

1.5.2. Specific objectives

- Preparation of cDNA display molecules from VHH DNA library
- Immobilization of gliadin protein on magnetic beads.
- Affinity selection of naïve VHH library against gliadin protein.
- Affinity confirmation of selected VHHs using cD-iPCR.
- Confirmation of the cD-iPCR results with pull-down assay and ELISA.
- Gliadin detection of commercial food samples using cD-iPCR.

1.5.3. Overall objective

To demonstrate potential application of immunization-free affinity antibody preparation technologies such as cDNA display method and cD-iPCR which reach the ethics and principles of modern scientific experimentation, especially in terms of animal protection.

Chapter 2

In vitro selection of anti-gliadin single-domain antibodies from a naïve library using cDNA display method

2.1. Introduction

Genotype-phenotype linking technologies such as phage display have been widely applied for selection of functional peptides and proteins. Recently, in vitro display technologies that are used with a cell-free translation system have become more promising because of their huge library size (~10^{13}) and incorporation of non-natural amino acids to peptides (Yamaguchi *et al.*, 2009). cDNA display is a new version of mRNA display that is one of the simplest genotype-phenotype linking methods (Yamaguchi *et al.*, 2009; Mochizuki *et al.*, 2011, Mochizuki et al., 2015). cDNA display is more stable than other in vitro display methods because cDNA is fused to its coding polypeptide covalently via a puromycin molecule. In addition, the cDNA display method is an immunization-free *in vitro* selection tool which is important when comes to obtaining antibodies that can recognize targets which cannot be used in immunizing animals due to their low immunogenicity or toxicity. In the following study, we used naïve VHH library prepared from non-immunized animals and the study aimed to select VHH antibodies against wheat gliadin. Since gliadin is not immunogenetic in all animals, it is difficult to ensure the formation of suitable antibodies by immunization techniques. Besides, some studies have indicated that the immunological response to antigen vaccines in children, even those with CD, does not differ markedly from that of the general population. Hence, *in vitro* selection techniques are necessary for screening antibodies against variable toxins, such as gliadin. The chapter two describes the development of high affinity

gliadin binding antibodies using cDNA display method which may use in gluten detection in the analysis of different gluten-free foods in future advancements.

2.2. Chemicals and instruments

The chemicals for the molecular biology experiments were obtained from Sigma Aldrich (MO, USA) and Thermo Fisher Scientific (MA, USA). Dynabeads MyOne C1 streptavidin beads and carboxylic acid beads were purchased from Invitrogen (CA, USA). DNA oligos and plasmids were synthesized by Eurofins Genomics (Tokyo,Japan). *In vitro* RNA transcription was performed using an *in vitro* transcription kit (T7 RiboMAX Express Large-Scale RNA Production System, Promega (WI, USA) and purified using a RNA purification kit (Hilden, Germany). DNA was purified using a FavorPrep PCR Clean-Up Mini Kit by Favorgen (WA, Australia). UV irradiation of the cnvK-puromycin linker was performed with a CL-1000 UV Crosslinker (UVP, CA, USA). The *In vitro* translation reaction was performed using a translation kit (Rabbit Reticulocyte Lysate Translation Systems, Promega (WI, USA)). End point PCR was performed with a Biometra TRIO48 thermal cycler. Unless otherwise stated, PrimeSTAR HS DNA polymerase (Takara, Japan) was used for PCR under the conditions recommended by the manufacturer. Electrophoresis analysis of DNA and RNA was performed at 60°C using 8 M urea containing 4% denaturing polyacrylamide gel electrophoresis (PAGE), with 0.5× TBE as a running buffer. SDS-PAGE analyses were performed at room temperature using Tris-HCl and gels with or without urea. All the DNA and RNA were stained with SYBRGold Nucleic Acid Gel Stain (Life Technologies, MD, USA). Gel images were taken with a Typhoon FLA9500 imager (GE Healthcare, Uppsala, Sweden). Band intensities were calculated using Quantity One 1-D Analysis Software Version 4.6.6. All chemicals, reaction buffer compositions and DNA fragment sequences/primers used in the study and abbreviation list are provided in the Annex I.

2.3. Methodology

2.3.1. Preparation of gliadin immobilized Beads

Gliadin from wheat (Sigma G3375), extracted as 1 mg/mL in immobilization buffer containing 70% ethanol (Annex I Table 1) was centrifuged at 10^4 g to remove undissolved particles. Carboxylic acid magnetic beads were activated for protein binding with N-hydroxysuccinimide (NHS) and 1-ethyl-3-(3-dimethylaminopropyl) carbodiimide hydrochloride (EDC) in MES buffer (25 mM, pH 6) and the proteins were immobilized according to the manufacturer's instructions. Beads were blocked with 5% (w/v) skim milk dispersed in 1× binding buffer (Annex I Table 1) for 1 h prior to each experiment. The yield of the immobilization reaction was estimated by measuring the protein concentrations of the solution before and after immobilization using a NanoDrop, and also by comparing the band intensity ratios on SDS-PAGE.

2.3.2. Construction of VHH-coding DNA library

Lymphocytes (around 2×10^7 cells/head) were isolated from the blood of 11 alpacas. Total RNA was extracted with TRIzol™ Reagent (Thermo Fisher Sci.) and one-tenth of it was used to synthesize cDNAs , and the synthesized cDNAs were amplified using VHH specific primers (Alp-Sfi-VHH-F1, Alp-Sfi-SHinge-R, Alp-LHinge-R) (Annex I Table 3). Using the generated VHH cDNA as a template, two gene fragments of CDR1-2 region or CDR3 region were amplified by PCR, and each amplified fragment was subjected to overlap PCR (Alp-FR3-overlap-F, Alp-FR3-overlap-R). The shuffled VHH gene were cloned into a phagemid vector and expressed as pIII fusion protein on the surface of a M13 filamentous phage. The resulting phage display VHH library was amplified in the Escherichia coli HST02 strain, cultured, and harvested by polyethylene glycol (PEG) precipitation before panning. Briefly, the culture was centrifuged (14000g for 20 min) and the supernatant was transferred to a new centrifuge bottle. A solution of PEG/NaCl (5×, PEG-6000

20% w/v, NaCl 2.5 M) was added to the supernatant and the mixture was incubated on ice for 1 h. The solution was again centrifuged, and the white phage pellet was resuspended in 10 mL of suspension buffer (PBS containing 10% glycerol). Transformants in the library were evaluated, by plating on 2xYT selective medium (100 mg/mL ampicillin), for library size.

2.3.3. Construction of protein-coding DNA full construct

Recombinant VHH DNA fragments were designed with the DNA fragments consisting of a T7 promoter, omega (Ω) enhancer, Kozak consensus sequence, VHH gene, His-tag, and linker hybridization region (Y tag) (summarized in Annex I Table 2). A schematic illustration of the DNA full construct for cDNA display harboring VHH gene is shown in Figure 2.1. The obtained full-length, VHH DNA library was used in the subsequent assays. Recombinant VHH DNA fragments for in vitro selected three VHH clones were also prepared in same manner as described above. The DNA construct of Anti-GFP VHH and BDA were prepared as described in Anzai et al, 2019.

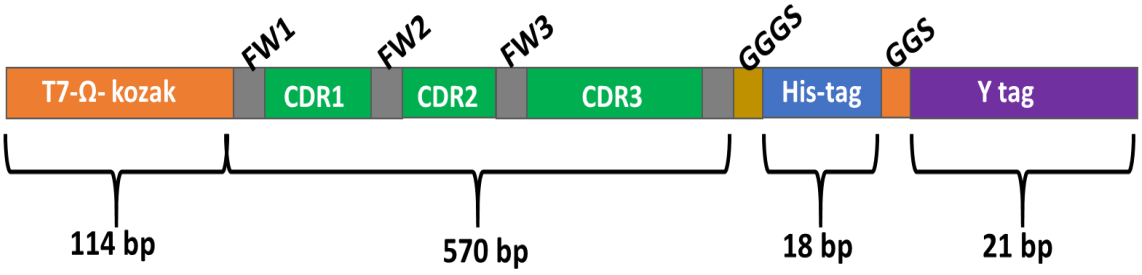

Figure 2.1. Full construct of the VHH DNA library. Recombinant VHH DNA fragments were designed with the DNA fragments consisting of a T7 promoter, omega (Ω) enhancer, Kozak consensus sequence, VHH gene, His-tag, and linker hybridization region (Y tag).

2.3.4. Synthesis of VHH cDNA display molecules

VHH cDNA display molecules were prepared according to our previously developed method with slight modifications (Yamaguchi *et al.*, 2009; Ueno and Nemoto, 2012). The full-length, VHH-coding DNA library was transcribed into a mRNA library. Transcription of DNA was performed with a T7 RiboMAX Large Scale RNA Production System (Promega) according to the manufacturer's instructions, and mRNA was purified by Agencourt RNAClean XP (Beckman Coulter). mRNA (1 μM) was then hybridized to cnvK-rG linker (1 μM) at the 3'-terminal region in 25 mM Tris-HCl (pH 7.5) with 100 mM NaCl under the following annealing conditions: heating at 90°C for 1 min followed by lowering the temperature to 70°C at a rate of 0.4°C/s, incubating for 1 min, then cooling to 25°C at a rate of 0.08°C/s (Mochizuki et al., 2015; Tanemura et al., 2015). The sample was irradiated with UV light at 365 nm using CL-1000 UV Crosslinker (UVP, Upland, USA) for 30 s. The obtained mRNA-linker complex was then in vitro translated with a rabbit reticulocyte lysate system (Promega, 6 pmol of mRNA-linker was added in 50 μL reaction volume) at 30°C for 20 min. To synthesize an mRNA−linker−protein fusion (i.e. mRNA display or IVV), KCl and $MgCl_2$ were added to the mixture (final concentrations were 900 mM and 75 mM, respectively), and the mixture was incubated at 37°C for 60 min. After incubating 5 mins at 37°C with EDTA (final 70 mM) and an equal volume of 2× SA binding buffer (20 mM Tris-HCl, pH 7.4, 2 mM EDTA, 2 M NaCl, 0.2% (v/v) Tween 20) was added, the mRNA display was immobilized on streptavidin (SA)-coated magnetic beads (Dynabeads MyOne streptavidin C1 streptavidin magnetic beads, Invitrogen, 60 μL) at 25°C for 30 min. The beads were washed three times with 1× SA binding buffer (100 μL, 10 mM Tris-HCl, pH 7.4, 1 mM EDTA, 1 M NaCl, 0.1% (v/v) Tween 20). The immobilized mRNA display was then reverse transcribed to form cDNA display using reverse transcriptase (Toyobo, Japan, 200 U in 50 μL reaction volume) at

42°C for 30 min. The beads were washed with His tag binding buffer (100 µL, 20 mM sodium phosphate buffer, 0.5 M NaCl, 5 mM imidazole, pH 7.4), and RNase T1 (Thermo Fischer Scientific) was added (250 U in 50 µL of His tag binding buffer) to the beads. The mixture was incubated for 30 min at 37°C to release the mRNA/cDNA−protein fusion molecules (i.e. cDNA display) from the beads. Supernatant containing cDNA display molecules was collected, and purification using 6×His peptide tag was performed to remove the contaminated cDNA-linker complex as follows. To His Mag Sepharose Ni beads (20 µL, GE healthcare) the above supernatant was added, and incubation was performed at 25°C for 2 h. The beads were washed with His tag wash buffer (100 µL, 20 mM sodium phosphate buffer, 0.5 M NaCl, 20 mM imidazole, pH 7.4), and incubated in His tag elution buffer (20 µL, 20 mM sodium phosphate buffer, 0.5 M NaCl, 250 mM imidazole, pH 7.4) at 25°C for 15 min. (Figure 2.2). The presence of the cDNA display molecules in elution sample was confirmed by a FITC check using a Nanodrop and the eluted fraction was used for assays after appropriate dilutions.

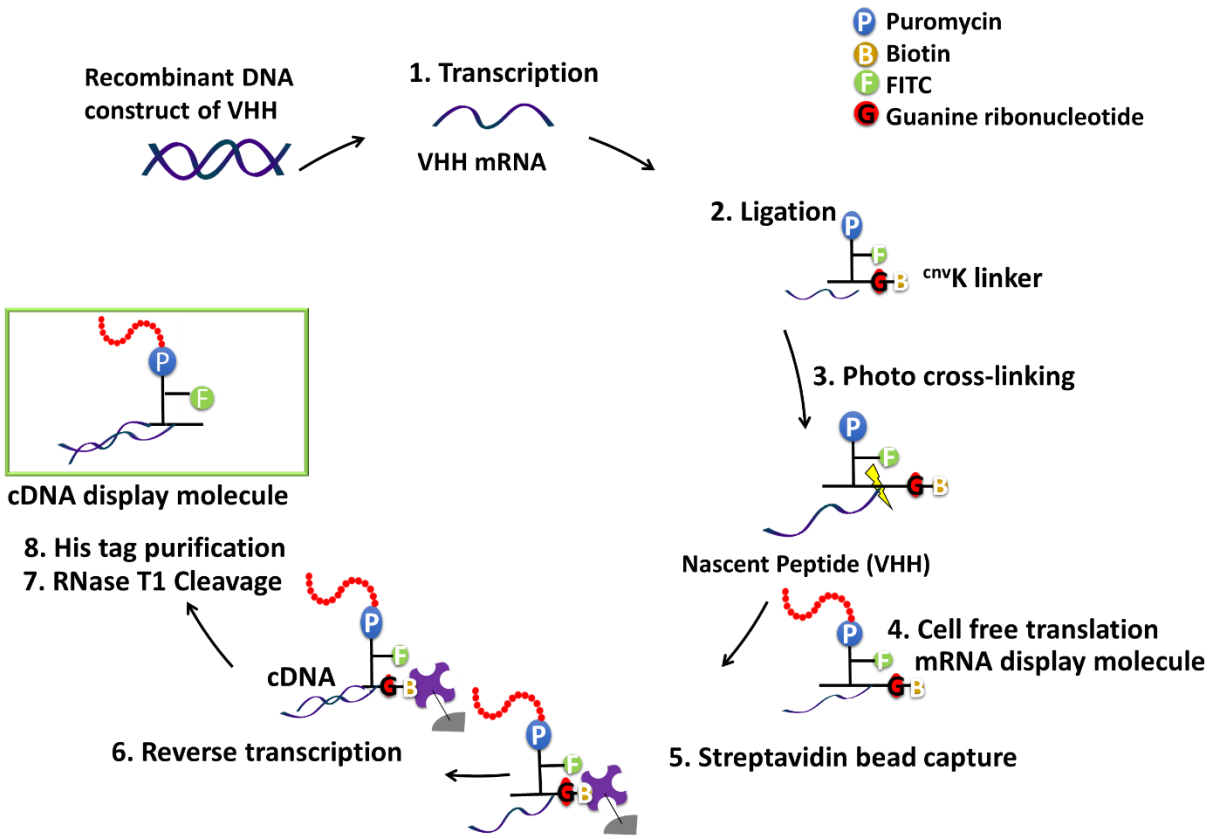

Figure 2.2. Preparation of cDNA display (schematic representation). The DNA library encoding VHH is transcribed into mRNA. An mRNA is photo cross-linked with Puromycin-linker. The cross-linking product is in vitro translated. The translated mRNA-protein fusion is immobilized onto SA beads for purification. The immobilized fusion is reverse transcribed to form an mRNA/cDNA-protein fusion (cDNA display molecule). The cDNA display molecule is released from SA beads by RNase T1 digestion and purified by His-tag purification.

2.3.5. Confirmation of cDNA display formation of VHH by SDS-PAGE

The VHH cDNA display molecules were prepared from 12 pmol of the mRNA–linker complex as described above in Section 2.3.4. Sample aliquots corresponding to 0.5 pmol from the mRNA–cnvK puromycin linker, mRNA display, elution of RNase T1 treatment (crude cDNA display), supernatant of SA-bead immobilization, and supernatant of His-tag purification were analyzed,

together with the purified cDNA display (10 pmol scale for clear visualization) using 8 M urea containing 4% stacking and 6% separating gels on SDS-PAGE. The loading amounts of the samples were calculated assuming that every step proceeded with perfect yield. The last three samples were incubated with RNase H before loading to the gel to avoid the entanglement with RNAs. The fluorescent marker attached to the linker was visualized by FITC scanning, and the band intensity ratios were compared after adjusting all samples to correspond to 0.5 pmol of molecules. The efficiency of the cDNA display formation was estimated from the ratio of the mRNA–linker and purified cDNA display band intensities.

2.3.6. *In vitro* affinity selection

A schematic representation of the in vitro selection cycle is given in Figure 2.3. Gliadin-immobilized magnetic beads (prepared in Section 2.3.1) were used after gradual 10-fold dilutions with intact beads in each selection cycle (40 to 0.04 µg/mL), to increase the severity of the selection and thereby improve the affinity and specificity. Counter selection was performed prior to each screening with intact carboxylic beads to avoid non-specific binding. The purified VHH cDNA display library (prepared in Section 2.3.4) was incubated with gliadin-immobilized magnetic beads for 1 h at 25℃ in a thermo block rotator. Unbound or slightly bound VHHs were washed away with 1× binding buffer containing 0.05% Tween 20 (BB-T) and the tightly bound display molecules were eluted with SDS/DTT elution buffer (see Annex I Table 1 for buffer composition) at 50°C for 30 mins (the in vitro selection conditions for each selection cycle are given in Table 2.1). The eluted DNA was purified into 40 µL of ultra-pure distilled water (UPDW) and amplified with VHH specific primers (forward primer: Newleft-F, reverse primer: cnvKpolyA-R) (see Annex I Table 3 for primer sequences) to generate the VHH DNA library for the next selection

cycle. The flow-through DNA, washed-away DNA, and eluted DNA were visualized on PAGE and the band intensities were compared.

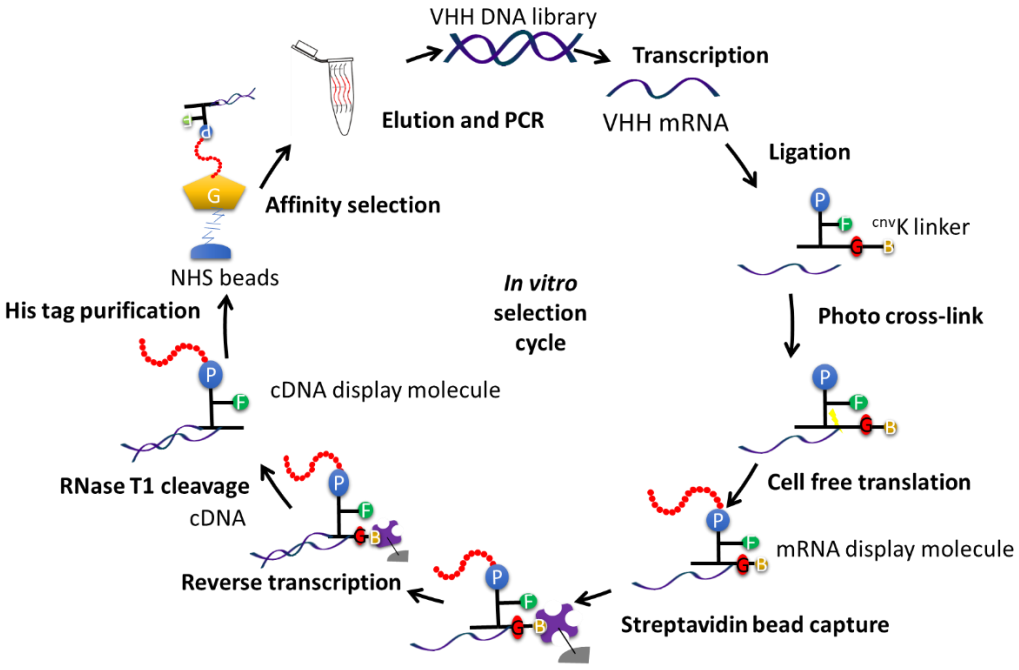

Figure 2.3. Schematic representation of cDNA displays in vitro selection. After preparing the cDNA display molecules, the purified cDNA display, which binds to immobilized target gliadin molecules, is amplified by PCR.

The binding VHH library was enriched for up to five continuous selection cycles, and negative selection was also performed in parallel using intact beads. Following the in vitro selection, NGS data analysis was performed under the conditions recommended by the manufacturer with nine sets of VHH DNA, including five positive selection libraries and four negative selection libraries obtained after each selection round.

Table 2.1. *In vitro* affinity selection conditions.

Round	cDNA Display (pmol)	Target (μg/mL)	Counter selection	Washing	
1	90	40	-	100 μL × 3	30 sec
2	12	4	Yes	100 μL × 3	30 sec
3	6	0.4	Yes	100 μL × 5	2 mins
4	6	0.04	Yes	100 μL × 7	3 mins
5	6	40	Yes	100 μL × 3	30 sec

2.3.7. Next Generation Sequence analysis (NGS)

NGS analysis was performed according to the respective analysis company guidelines (Illumina Inc., Shiba, Minato-ku, Tokyo). A total of 9 sets of VHH DNA including five positive selection libraries and four negative selection libraries obtained after each rounds of in vitro selection were analyzed using a MiSeq system. The MiSeq library for VHH DNA sequencing was prepared using Illumina Nextera XT chemistry (Illumina) following the protocol provided by the manufacturer. DNA pool generation for Illumina sequencing Barcodes were attached by PCR to the pools of all selection rounds. The genes from the VHH library were amplified in 2 steps, firstly using the pre-adaptor primers (prRd1N4VHH-F and prRd2N4VHH-R) and secondly with sequence specific forward primers for each selection round including negative selection rounds (prNexteraXTIndex1(N701) to prNexteraXTIndex1(N709)) and reverse primer (prNexteraXTIndex2(N501), respectively (see Annex I Table 8 for primer sequences). The final loading concentration was adjusted to 10 nM following the MiSeq loading protocol. The

sequencing data was converted into amino acid sequences and the data was aligned using Genetix and Excel softwares. Low-quality sequencing data were first trimmed depending on quality and reads with less than 100 amino acids in length. The cleaned-up sequencing data were summarized and counted. The most frequently occurring sequences (~3.8 %) were considered and the CDR regions were compared with the library and also negative selection sequences to check the enrichment. Three highest occurrence frequencies which fulfil all the above requirements were selected as candidate VHHs and the corresponding DNA sequences were synthetically generated (Eurofins Genomics, Japan) as described in Section 2.3.3.

2.3.8. Pull-down assay with cell-free translation for VHH candidates

Three pull-down assay experiments were performed using a puromycin linker. Cell-free translated protein-linker complex was used as the pray protein (Nemoto *et al.*, 2014). In all assays, 12 pmol of the cross-linked product was translated to synthesize the mRNA–linker-protein fusion molecules, as described previously in Section 2.3.4. The formed fusion molecules were captured using streptavidin magnetic beads and washed with 1× binding buffer. RNase H was added to degrade the mRNA portion of the mRNA–linker-protein fusion molecules, and also to release the complex (i.e. linker-protein fusion) from the magnetic beads. Eluted protein-linker complex was then incubated with target-immobilized magnetic beads (Gliadin, IgG or GFP) for 1 h at 25°C in a thermos block rotator. After three washes with 1× BB-T, the residual prey proteins were eluted with SDS/DTT elution buffer at 50°C for 30 min. After incubating at 90°C for 5 min with 1× SDS-PAGE sample buffer, the elutes were analyzed using 8 M urea containing 4% and stacking 12% separating gels on SDS-PAGE. The FITC-labeled VHH proteins were visualized using a fluorescence imager.

In the first assay the VHH protein-linker complexes were incubated with gliadin-immobilized magnetic beads (Gliadin-immobilized magnetic beads were prepared as in Section 2.3.1). After analyzing the input, flow-through, and elute on SDS-PAGE, the band intensities of were determined for each VHH1, VHH2 and VHH3 candidates (Figure 2.9A). The binding percentages and recovery percentages were calculated based on the band intensities.

In the second assay (Figure 2.9B), three candidate VHH elutes (after the incubation with gliadin-immobilized magnetic beads) were compared with the initial library to confirm enrichment of binders.

In the third assay (Figure 2.10), specificity of the selected VHH1 towards gliadin was compared with other two protein coding cDNA displays (anti-GFP VHH and B domain of protein A (BDA)) and also with empty beads. The DNA construct coding BDA and anti-GFP VHH were prepared according to our previous paper (Anzai *et al.*, 2019b). Cell-free translated protein-linker complex was prepared in same manner mentioned above in section 2.3.4 and IgG and GFP immobilized magnetic beads were prepared as in Section 3.3.1 and 3.3.2 respectively.

2.3.9. Expression of VHH proteins

VHH-encoding DNA was cloned downstream of a promoter in an expression vector (in house-build pPANA-02 vector) using the appropriate restriction enzymes. The vector was then introduced into a host cell DH5α and the insertion of the DNA was confirmed by colony PCR. Cell-transformed plasmid vectors, isolated from positive clones, were purified and again transformed into BL21 (DE3) for the protein expression. The VHH fragments with 6 × His-tag after expression were obtained by purifying the cell lysates with Ni-NTA affinity columns. The size of the purified VHHs was determined using 6% stacking and 12% separating SDS PAGE (Figure 2.12).

2.3.10. ELISA for candidate VHHs

The binding ability and the specificity of the expressed candidate VHHs were estimated by performing an indirect ELISA. ELISA plates (Nunc MaxiSorp® flat-bottom 96 well plate, Thermo Fisher Scientific, MA, USA) were coated with 50 µL of 10 µg/mL gliadin and 10 µg/mL BSA separately overnight at 4°C. After blocking the wells with 5% skimmed milk-PBS for 1 h, 50 µL of serial dilutions of VHHs (10 to 0 µg/mL) were added to both the gliadin- and BSA-coated plates and incubated for 1 h. After washing 5 times with 200 µL PBS-T, 50 µL of a 1/5000 dilution of Monoclonal ANTI-FLAG® M2-Peroxidase (HRP) antibody was added and incubated for 1 h. After washing 6 times with 200 µL PBS-T, the peroxidase activity was developed by adding 50 µL of peroxidase substrate (1 mg/mL *o*-phenylenediamine dihydrochloride-2HCl, 0.01% H_2O_2 in 0.1 M NaH_2PO_4; pH 5.5) and incubating 5 min at room temperature. The enzyme reaction was stopped by adding 50 µL of 1 M H_2SO_4, and the absorbance was measured at 450 nm. Previously optimized anti-BSA antibody (unpublished data) was used as a negative control in the gliadin-coated plate and as a positive control in the BSA-coated plate.

2.4. Results and Discussion

2.4.1. Target Immobilization

First, gliadin protein was immobilized on the magnetic beads. Commercialized gliadin that was not separated into α/β, and γ subcategories was used as the starting material to select VHH proteins that recognize total gliadin in food samples. Protein was extracted using 60 % ethanol and immobilized. Protein immobilization on NHS activated magnetic beads was confirmed by SDS-PAGE. Input gliadin protein, the flow-through after incubation with NHS beads and the wash away samples were tested on SDS-PAGE. Comparison of the band intensities of input gliadin (all bands in 30~70 kDa) and the flow through after immobilization indicated that approximately 70% of the

gliadins were immobilized on the beads. The last wash showed a very low band intensity indicating adequate retention of gliadin on the beads (Figure 2.4).

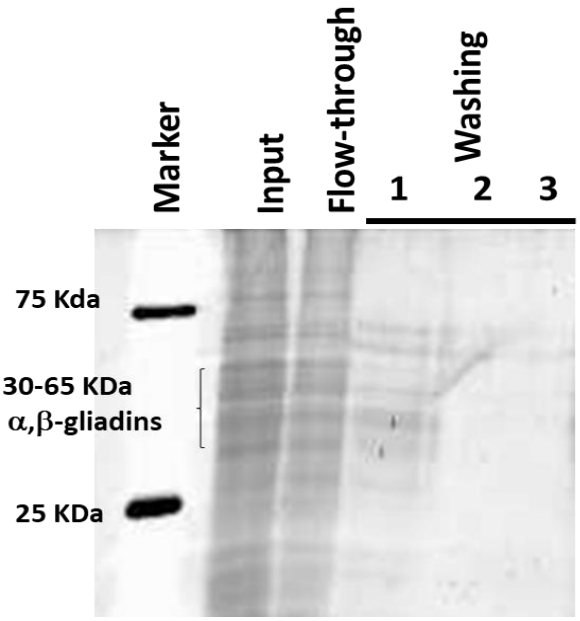

Figure 2.4. Gliadin immobilization confirmation on the SDS PAGE. Comparison of the band intensities of input gliadin (all bands in 30~70 kDa) and the flow through after immobilization indicated that approximately 70% of the gliadins were immobilized on the beads.

2.4.2. Confirmation of VHH cDNA display molecule formation on SDS-PAGE

A DNA library encoding VHH was prepared as described above and transcribed in vitro to yield mRNA. The mRNA was annealed to the puromycin linker and photo-crosslinking was performed. The cross-linking efficiency of the puromycin linker with the mRNA was estimated to be more than 90% according to the band intensity ratios visualized on PAGE analysis (Figure 2.5). Because fluorescein is attached to the puromycin linker, only the cross-linked mRNA (and unbound linker) is visualized using a FITC filter. It should have more that 80%-90% of ligation of the linker to mRNA because remaining free linkers in the protein translation solution may end up inefficient cDNA display formation.

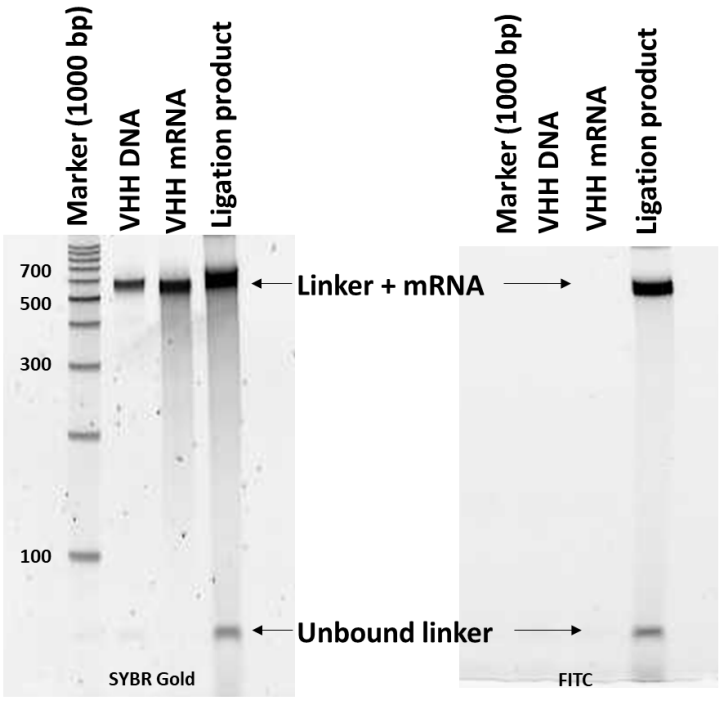

Figure 2.5. Cross-linked VHH DNA and puromycin linker visualized in denaturing PAGE with SYBER gold stain (left) and FITC scan (right). Lane 1: 100 bp DNA ladder, Lane 2: VHH DNA (570 bp), Lane 3: VHH mRNA, Lane 4: cross-linked product.

Next, cDNA display was formed from the cross-linked mRNA according to the procedures established (Yamaguchi *et al.*, 2009; Ueno and Nemoto, 2012). The successful formation and purification of cDNA display molecules was confirmed by detecting fluorescein attached to the puromycin linker on SDS-PAGE (Figure 2.6). Lane 1 was the puromycin linker connected to the VHH mRNA and this was used as the reference to compare all samples applied. Any marker compound was not used, because as the cDNA display molecules were DNA/protein complexes, the band positions did not match well with any standard markers. In Lane 2, the upper band was the formed mRNA/protein complex or the mRNA display molecule and the lower band corresponded to the mRNA-linker that was not conjugated to a peptide. Lane 3 indicated the unpurified cDNA display molecule after RNase T1 cleavage. Lanes 4 and 5 displayed the

supernatants after SA bead immobilization and Ni-NTA bead immobilization respectively. The low intensity of these bands indicated that immobilization was successful. Purified cDNA display molecules were applied into lane 6 with a higher concentration (10 pmol) to achieve better visualization on SDS-PAGE, because the formation yield of display molecules appears to be low as indicated from previous experience. The formation efficiency of the cDNA display molecules was calculated as 5.6% from the band intensity ratio of Lane 1 and Lane 6.

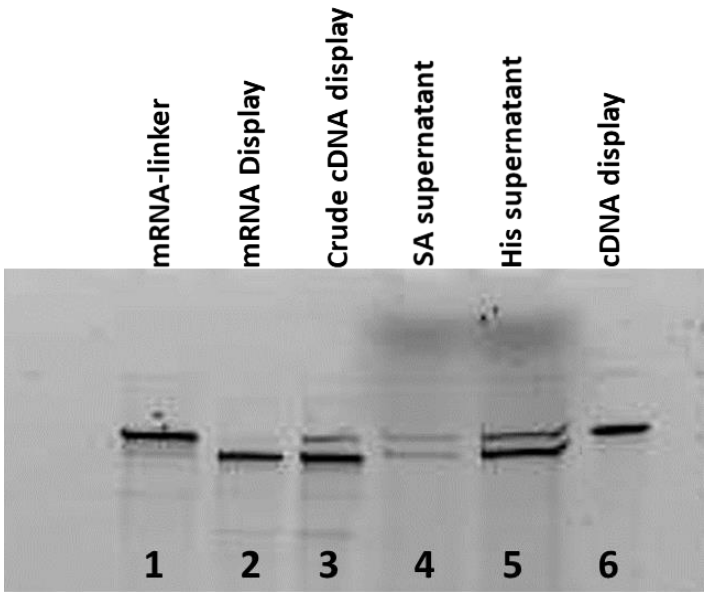

Figure 2.6. Confirmation of cDNA display formation of VHH DNA. Lane 1: the puromycin linker connected to the VHH mRNA, Lane 2: the formed mRNA/protein complex. Lane 3: the crude cDNA display molecule, Lanes 4 and 5: the supernatants after SA bead immobilization and Ni-NTA bead immobilization, respectively, and Lane 6: the pure cDNA display molecules.

2.4.3. *In vitro* affinity selection of VHH against gliadin

Using the cDNA display library, five rounds of in vitro selection was performed against gliadin-bound beads. As shown in Table 2.1, the immobilized gliadin concentration was reduced by 10-fold in each selection round to increase the selectivity of the binders. Following the incubation, the severity of the washing was also increased to obtain high affinity VHHs. Figure 2.7 shows a comparison of the band intensities of VHH DNA in flow through and elution. When the number of selections was increased the elute quantity was also increased and reached a plateau, indicating enrichment of the binders. In Figure 2.8, the band intensities of the 5^{th} selection round are graphically compared with the parallel negative selection band intensities. The intensity of the positive selection elution band (E1, left) was considerably higher (by approximately 11-fold) than the negative selection elution band (E1, right). This result indicated high specific and low nonspecific binging of candidate VHHs. All the selection elutes were analyzed by NGS, instead of analyzing the last selection elute only, to generate more comparable sequence data. According to the percentage abundance (frequency) of the NGS data, the top three VHH sequences, which were not appeared in the negative selection data pool were selected as candidate VHH sequences. The amino acid sequences of the selected VHHs are given in Table 2.2 and Annex I Table 4.

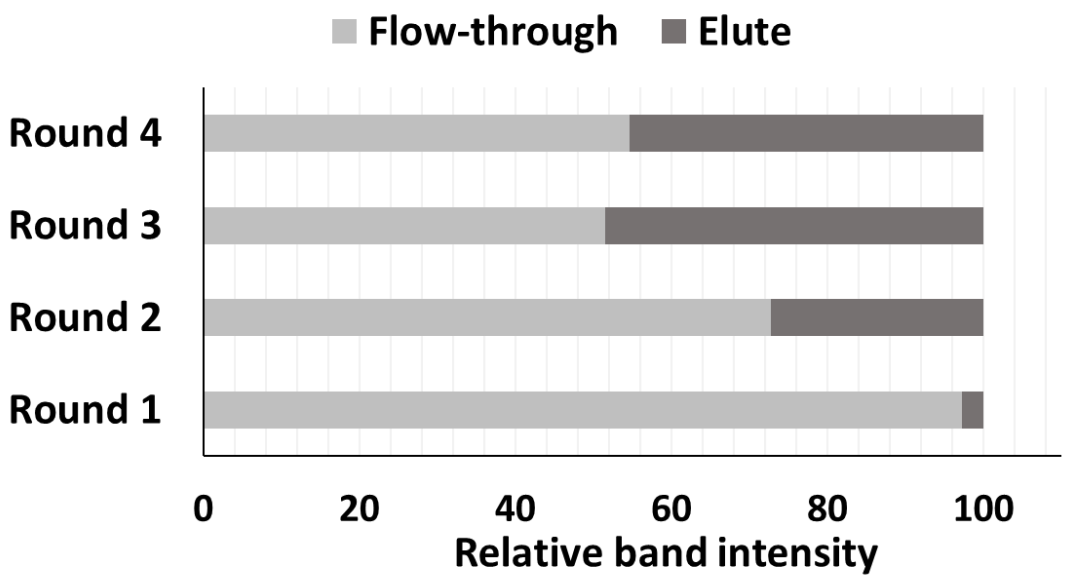

Figure 2.7. Comparison of band intensity ratios during selection rounds 1–4.

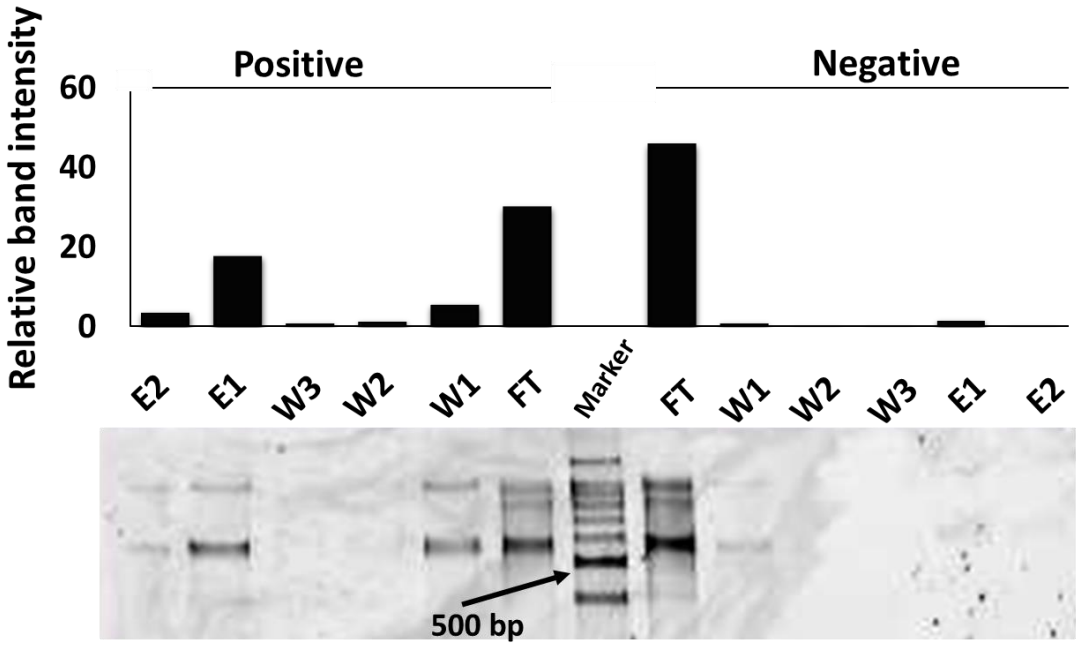

Figure 2.8. Comparison of the band intensities of positive (left) and negative selection (right) of the 5th selection round.

Table 2.2. The CDR region sequences of selected VHHs.

ID	CDR 1	CDR 2	CDR 3	AA
VHH1	DRTFSNYSMG	ITHNGSTNFPD	AVDHSFITVVRGEEDLE	135
VHH2	GPEWRHYHMG	ISWSGGTTMYAD	AAGDTVVALLDYRAY	134
VHH3	ATIFGSNSMA	TVARNGNTGYVD	NLKRYRMGFILDGDY	133

2.4.4. Pull-down assay for candidate VHHs

Three pull-down experiments were performed to confirm the binding of selected VHHs toward gliadin in the format of linker-protein fusions. In assay one, the binding percentage of each VHH toward immobilized gliadin was calculated by the ratio of the input and flow-through band intensities (Figure 2.9A). VHH1 and VHH2 appeared to bind with high affinity (18% and 12% binding percentages, respectively), which was ~10-fold higher than VHH3 (2%). The recovery percentages were also calculated from the ratio of input and recovery band intensities and there, lower recovery percentages were observed than the binding percentages. This may be due to incomplete elution of bound molecules with 1% SDS and 50 mM DTT. However, the recovery data also indicated the same pattern of binding, with VHH1 and VHH2 exhibiting higher affinity toward gliadin compared with VHH3 (Figure 2.9A).

The binding ability of candidate VHHs was also compared with the initial VHH library (Figure 2.9B). The band intensities of the candidate VHHs were considerably higher (Lanes 1–3) compared with the initial library (Lane 4). These data confirmed the enrichment of the gliadin binging VHHs during the *in vitro* selection.

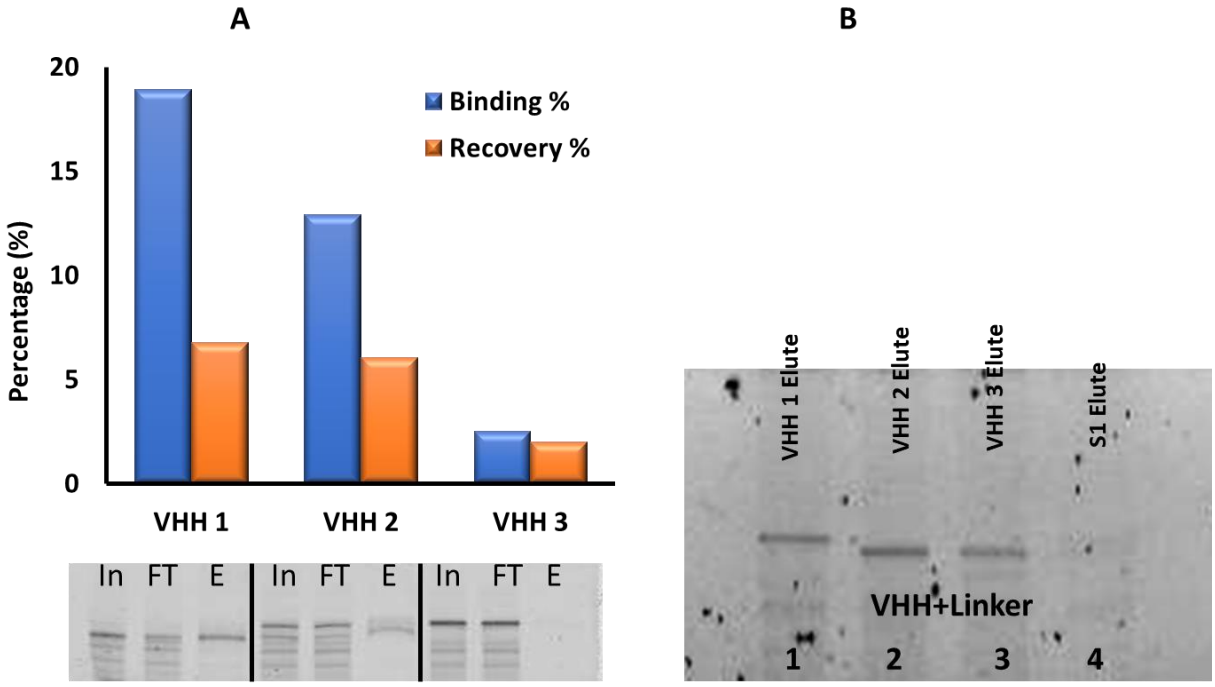

Figure 2.9. Pulldown assay results of candidate VHHs. A) The binding rate and recovery rate of each VHH toward gliadin in the pull-down assay. B) Comparison of the VHH binding to gliadin with the initial library. Lanes 1, 2, and 3: VHH1, VHH2, and VHH3, respectively. Lane 4: initial VHH library.

Thirdly, a pulldown assay was performed to confirm the specificity of the selected VHHs towards gliadin in comparison with control proteins (Figure 2.10). VHH1, which had higher affinity compared to other two VHHs, was used in the assay. As negative control proteins previously confirmed anti-GFP VHH (a protein that binds to Green Fluorescent Protein (GFP)) and BDA (a

protein domain that binds to Immunoglobulin G (IgG) protein) were used (Anzai *et al.*, 2019). They are both single chain peptides and able to form linker-protein fusions with puromycin linker. The assay results indicated the specific binding of VHH1 towards gliadin (Figure 2.10, Lane 1), and almost no binding to IgG, GFP or empty beads (Lane 2, 6, and 5, respectively). Also, the results confirmed that the control proteins BDA and anti-GFP VHH showed specific binding to IgG and GFP, respectively (Lane 4 and 7), and that gliadin immobilized beads did not show binding to control protein BDA (Lane 3). The results indicate that the band of BDA (eluted from IgG-beads) was nearly 2-fold stronger than the other two proteins (compare Lane 4 with Lanes 1 and 7).

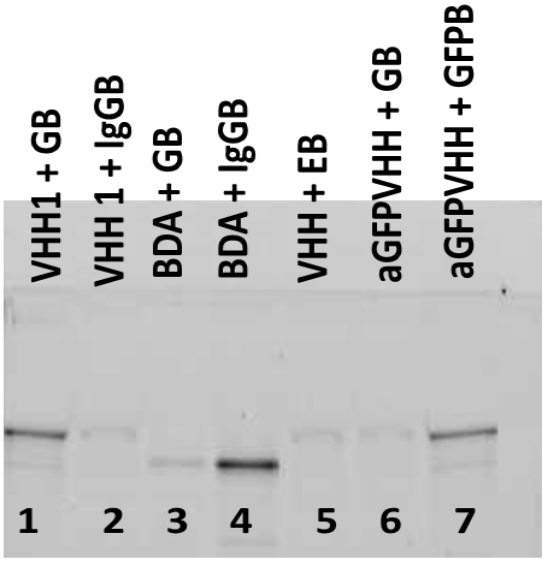

Figure 2.10. Binding specificity of VHH1 towards gliadin. Lane 1: anti-gliadin VHH + gliadin beads, Lane 2: anti-gliadin VHH + IgG beads, Lanes 3: BDA peptide + gliadin beads, Lane 4: BDA peptide + IgG beads, 5: anti-gliadin VHH + empty beads, Lane 6: anti-gliagin VHH + GFP beads and Lane 7: anti-GFP VHH + GFP beads. Only the elutes are shown.

According to previous results of the cDNA display related studies, the method is more compatible towards small peptides (<10 kDa) and larger proteins (>20 kDa) generally have lower cDNA display formation efficiencies (Yamaguchi *et al.*, 2009; Anzai *et al.*, 2019). So, the reason that the observed difference of band intensities was due to different input amount of linker-protein fusions. In short, the assays demonstrated that the VHH1 was specific for gliadin and the binding was not derived from potential stickiness of gliadin or selected VHH molecules.

2.4.5. Indirect ELISA for candidate VHHs

Next, VHH proteins were expressed with a FLAG tag in *E. coli* and estimated the affinity of expressed VHHs toward gliadin by indirect ELISA. In this experiment, VHHs were incubated with a target protein that was coated on plate, and the amount of bound VHHs were quantified by anti-FLAG antibody labelled with HRP. First, VHHs were reacted with gliadin to confirm the affinity (Figure 2.11A). As the graph shows, VHH1 and VHH2 clearly bound to gliadin in a concentration-dependent manner, and their signals were significantly stronger than VHH3 ($p < 0.01$, *t*-test). The original absorbance data was given in Annex I Table 6 for further confirmation. Anti-BSA VHH was also reacted with coated gliadin as the negative control, and the absorbance was not significant ($p > 0.01$ between 0 and 10 µg/mL, *t*-test), indicating that the binding of candidate VHHs towards gliadin was not due to potential stickiness of gliadin. Thus, the signals in the positive samples explained the VHH binding to gliadin.

Alongside, to measure the specificity of the VHH proteins toward gliadin, the second ELISA experiment was designed using BSA. Plates were coated with BSA protein and the assay was performed with VHHs, and an anti-BSA VHH as the positive control. As expected, the absorbance of the all the VHHs was significantly lower compared with the positive control ($p < 0.01$, t-test) indicating low nonspecific binding of selected VHHs (Figure 2.11B).

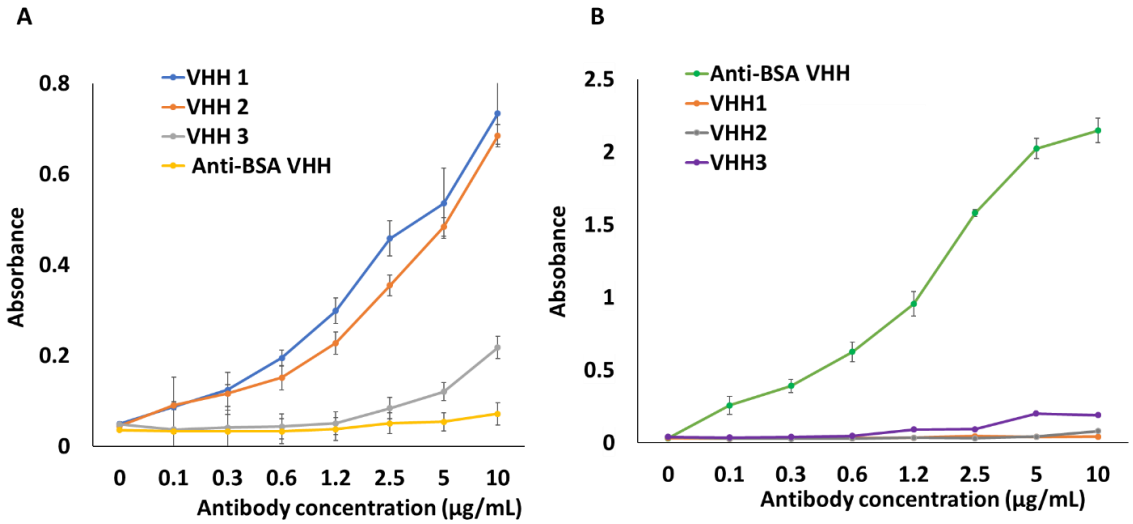

Figure 2.11. ELISA assay results of the candidate VHHs. (A) ELISA assay to determine the affinity of the candidate VHHs. Gliadin was used as the target, and anti-BSA antibody was used as a negative control. Data are shown as mean ± S.D. (n = 3). (B) ELISA assay to determine the specificity of the candidate VHHs. BSA was used as the target, and anti-BSA antibody was used as a positive control. Data are shown as mean ± S.D. (n = 3).

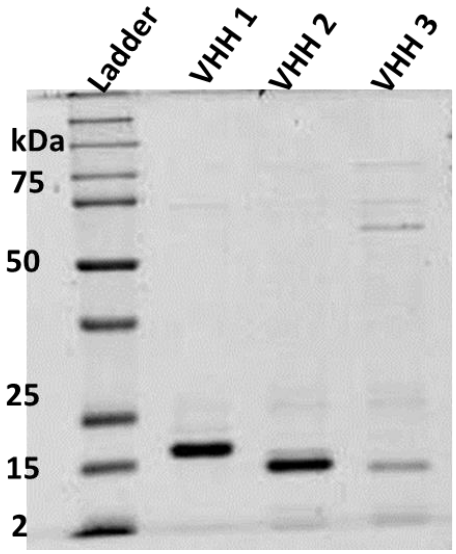

Figure 2.12. SDS-PAGE data for VHH protein expression. Lane 1: protein ladder, Lanes 2, 3, and 4: VHH1, VHH2, and VHH3, respectively.

2.5. Conclusions

Single domain antibody (e.g., Nanobody, VHH antibody) is a promising scaffold for therapeutic and diagnostic reagents. To expand the range of target molecules, in vitro selection using cell-free display technologies such as cDNA display is useful and powerful because of their huge libraries and robust stability. As discussed here, a naïve VHH DNA library was used successfully for selecting VHH candidates that specifically bound to toxic gliadin, without immunizing animals, using the cDNA display assay. The presence of several components in the gliadin protein mixture was a challenge as this might cause uneven immobilization of a the protein on the beads during each selection round. Based on NGS analysis data three candidate VHHs were selected at the end of the in vitro selection.

Chapter 3

Detection of gliadin using cDNA display mediated immune-PCR (cD-iPCR)

3.1. Introduction

The detection of specific biomarkers with high sensitivity is critical for early diagnosis and treatment. Immuno-PCR, often abbreviated as iPCR, is a well-established method in detection and quantification of low abundance biomarkers that exist in biological samples (*e.g.*, serum and urine). iPCR, which first requires labeling detection antibodies with DNA oligos and utilizing PCR to generate amplified signals correspond to an antigen binding reaction. (Sano *et al*., 1992). However, the conventional process of iPCR utilizes DNA-conjugated antibodies, chemical modification of antibodies which not only reduces antibody affinity but also creates a heterogeneous population of products (van Buggenum *et al*., 2016, Sano *et al*., 1992, Hendrickson *et al*., 1995). To overcome this problem, the covalent conjugates of aptamer/antibody-DNA fusion molecules can be used in the detection of multiple target biomarkers using real time immuno-PCR. The cD-iPCR, which takes an advantage of the structural characteristics of cDNA display is one of such which proved to work in detection of target proteins both in direct and sandwich-type formats (Anzai *et al*., 2019). cDNA display is one of the simplest genotype-phenotype linking methods, where cDNA is always covalently fused to its coding polypeptide (which can act as the affinity probe for the target) in 1:1 ratio via a uniquely designed puromycin linker (Yamaguchi *et al*., 2009; Mochizuki *et al*., 2011, Mochizuki *et al*., 2015). The cD-iPCR method is based on a covalent homogeneous DNA-antibody conjugation, non-viral, and almost a ready to use reagent in immune-detection assays. The following chapter is describing the application of newly developed cD-iPCR method in determining the affinity of selected VHHs against gliadin.

3.2. Chemicals and instruments

The chemicals for the molecular biology experiments were obtained from Sigma Aldrich (MO, USA) and Thermo Fisher Scientific (MA, USA). Real-time quantitative PCR (qPCR) was performed with a StepOne Real-Time PCR System. All chemicals, reaction buffer compositions and DNA fragment sequences/primers used in the study and abbreviation list are provided in the Annex I.

3.3. Methodology

3.3.1. Preparation of Immunoglobulin G (IgG) immobilized Beads

IgG from rabbit serum (Sigma, 1.5 nmol) in reaction buffer (0.1 M Na2HPO4, 0.1 M NaH2PO4, 0.3 M NaCl) was reacted with EZ-Link Sulfo-NHS-SS-Biotin (Thermo Fisher Scientific, 30 nmol) in reaction buffer at 25°C for 30 min, and then the buffer was exchanged to 1× SA binding buffer (10 mM Tris-HCl, pH 8.0, 1 mM EDTA, 1 M NaCl, 0.1% (v/v) Tween 20). Yield of collection was measured from absorbance at 280 nm of IgG. Dynabeads MyOne streptavidin C1 magnetic beads (Invitrogen, 20 µL) were washed with 1× SA binding buffer (100 µL), and reacted with the collected IgG (60 pmol) at 25°C for 30 min, then washed out by 1× SA binding buffer (100 µL, 3 times). Yield of immobilization reaction was estimated by subtracting the absorbance of IgG in the flow through from that in the input.

3.3.2. Preparation of Green Fluorescent protein (GFP) immobilized Beads

Carboxylic acid magnetic beads were activated for protein binding with N-hydroxy succinimide (NHS) and 1-ethyl-3-(3-dimethylaminopropyl) carbodiimide hydrochloride (EDC) in MES buffer and the GFP protein were immobilized as follows. NHS activated carboxylic beads were incubated with anti-GFP pAb (MBL, #598) for about one hour at 25°C and excess were washed away with

1 × binding buffer. Anti-GFP pAb beads were then incubated with GFP protein solution (known concentrations) for 2 h at 25°C. Beads were then washed with 1 × binding buffer for several times.

3.3.3. Determination of sensitivity using cD-iPCR

Determination of the sensitivity of VHHs toward gliadin was performed using our previously developed immuno-PCR method (cD-iPCR) with slight modifications (Anzai *et al.*, 2019). Gliadin immobilized-magnetic beads were diluted gradually in 10-folds steps with empty beads (0–10 µg/mL). Equal aliquots of purified cDNA display molecules of candidate VHHs were incubated with gliadin beads for 1 h at 25°C and after washing with 1× BB-T, the bound display molecules were eluted with SDS/DTT elution buffer at 50°C for 30 min. After the DNA was purified into 30 µL of UPDW, 5 µL of the template DNA was used for qPCR. The qPCR mixture contained template DNA, 1× Thunderbird SYBR qPCR Mix, a 300 nM concentration of each forward and reverse primers, 50× ROX reference dye, and UPDW. The step program for qPCR was set as 95°C for 1 min, followed by 40 cycles at 95°C for 15 s and 62°C for 35 s. A negative control that contained all the qPCR reagents, except the DNA template, was included to verify the quality of the amplification. The Ct value of the 0 ng/mL (no template beads) or qPCR negative sample (primer only) were subtracted from the other sample Ct value accordingly to calculate the ΔCt values.

3.3.4. Determination of the specificity using cD-iPCR

The DNA construct coding BDA and anti-GFP VHH were prepared according to our previous paper (Anzai *et al.*, 2019). The DNA constructs of VHH1, BDA and anti-GFP VHH were converted to cDNA display molecules according to the protocol described in Section 2.3.4. All the protein-coding cDNA display molecules of VHH1, anti-GFP VHH and BDA were incubated for 1 h at 25°C with each gliadin beads, IgG beads, GFP beads, or empty beads. All beads were then

washed with 1× BB-T, and the bound display molecules were eluted separately with SDS/DTT buffer at 50°C for 30 min. DNA was then purified and the qPCR was performed with the same conditions as described above in Section 3.3.3 with the respective primes (see Annex I Table 3 for primer sequences). The difference of the Ct values between the samples and the negative control (primer only) were calculated.

3.3.5. Determination of gliadin in the presence of other food components using cD-iPCR

A graphical illustration of the gliadin detection in food samples using cD-iPCR is shown in Figure 3.1. A short-grain cultivar of Japonica rice was used as the gluten-free food sample. The rice was ground into a fine powder and extracted for 2 h at 25°C in DMSO/PBS buffer (1:9 v/v). The extract was then centrifuged at 10^3 g for 15 min to separate the supernatant and subsequently diluted to 100 ng/mL with PBS buffer. Rice extracts and buffer samples (control) were spiked with a series of gliadin concentrations of 0 (gliadin-free control), 0.05, 0.5, and 5 ng/mL. First, the gliadin-spiked rice and buffer samples were incubated with equal aliquots of VHH cDNA display molecules for 1 h at 25°C. Then, the mixture was incubated with gliadin-immobilized magnetic beads (50 ng/mL) for 1 h to capture the remaining VHHs. Gliadin beads were then washed with 1× BB-T, and the bound display molecules were eluted with SDS/DTT buffer at 50°C for 30 min. DNA was then purified and the qPCR was performed with the same conditions as described above in Section 3.3.3. The difference in the Ct values between the samples and the negative control (primer only) were calculated.

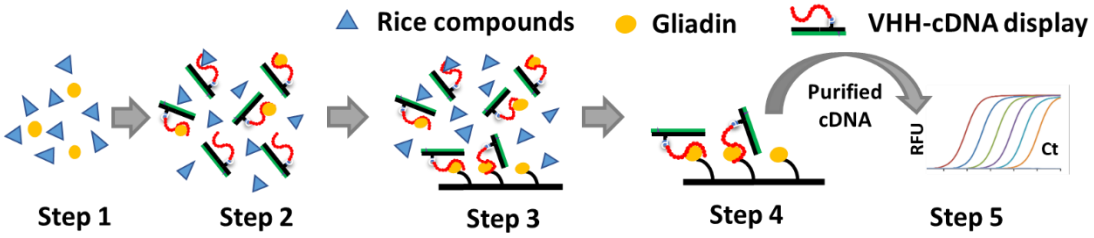

Figure 3.1. Graphical illustration of the gliadin detection in food using cD-iPCR. Step 1: Rice is spiked with gliadin, Step 2: Incubate VHH-cDNA display with the gliadin-spiked rice sample, Step 3: Incubate the mixture with immobilized gliadin, Step 4: Wash and elute the bound VHH-cDNA display, Step 5: Real-time PCR.

3.3.6. Extraction of gliadin from commercial food samples for cD-iPCR

Wheat flour, breadcrumbs, rice crackers, oats, potato starch and corn starch were purchased from local supermarket for gliadin detection. Gliadin fractions were extracted from food samples including sample control Sigma-Aldrich gliadin from wheat (G3375). The Sigma-Aldrich gliadin from wheat (G3375) 2 mg was dissolved in 250 µL of 60% (v/v) ethanol, incubated with gentle shaking at 100 rpm for 20 min at RT, and centrifuged for 20 min at 10 000× g. The supernatant was recovered. A sequential extraction procedure was adopted to separate albumins/globulins, gliadins in commercial food samples. Briefly, the albumins/globulins were extracted twice from 20 mg of powdered food sample with 1 mL of 0.4 M NaCl by incubation in an orbital shaker at ambient temperature with gentle shaking (100 rpm) for 20 min followed by centrifugation at 10,000 g for 20 min at room temperature. The gliadin fraction from the remaining pellet was extracted stepwise three times with 500 µL of 60% (v/v) ethanol, incubated with gentle shaking (100 rpm) for 20 min at room temperature, and centrifuged for 20 min at 10,000× g. Following centrifugation, the supernatants containing the gliadin fraction were collected and the presence of gliadin fractions was estimated by SDS-PAGE.

3.3.7. Detection of gliadin in commercial food samples using cD-iPCR

Gliadin fractions extracted from food samples (2 mg/mL) were immobilized on BcMag™ C-4 magnetic beads according to the manufacturer's instructions. Beads were blocked with 5% (w/v) skim milk dispersed in 1× binding buffer for 1 h prior to each experiment to avoid the non-specific binding. Equal aliquots of purified cDNA display molecules of candidate VHH1 were incubated with gliadin beads for 1 h at 25°C and after washing with 1× BB-T, the bound display molecules were eluted with SDS/DTT elution buffer at 50°C for 30 min. After the DNA was purified into 30 µL of UPDW, the qPCR was performed with the same conditions as described above in Section 3.3.3. The difference in the Ct values between the samples and the negative control (primer only) were calculated.

3.4. Results and discussion

3.4.1. Detection sensitivity using cD-iPCR

As an application of the selected VHH, we applied our previously developed cD-iPCR method to detect gliadin in samples. cD-iPCR is a novel format of immuno-PCR using cDNA display molecules, where the protein part (VHH in this case) is used for binding to the target and the cDNA part is used as a template for qPCR-based quantification. First, cDNA display molecules encoding three VHHs were incubated with a series of different concentrations of gliadin-immobilized beads and the threshold cycle (Ct) values were obtained after qPCR. The Ct value of the no gliadin (0 µg/mL) sample was subtracted from the Ct values of the other concentrations of gliadin to obtain the comparable results shown in Figure 3.2. The data showed a clear gradual increase in the ΔCt values with increasing gliadin concentrations. These results indicated that cD-iPCR of the selected VHHs could detect gliadin in the range of 0.001 to 10 µg/mL, with satisfactory statistical significance ($p < 0.01$, *t*-test). Among three VHHs, VHH1 and VHH2 appeared to have higher

affinity to gliadin compared with VHH3. The observed pattern of binding was similar to pull-down assays, confirming the accuracy of this method.

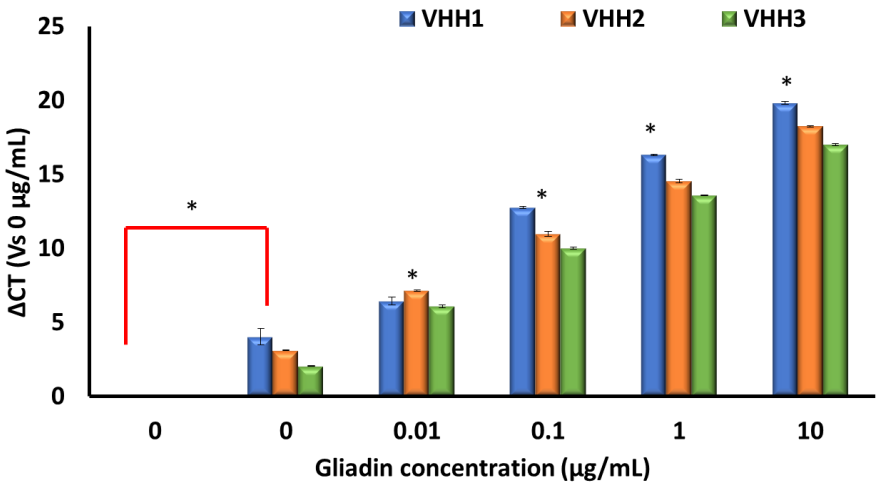

Figure 3.2. The cD-iPCR results of the VHH proteins binding with gliadin. (concentrations ranging from 0.001 to 10 µg/mL). * indicates $p<0.05$, n=3.

In Figure 3.3, the Ct value of the negative sample (primer only) was subtracted from the Ct values of the different gliadin concentrations, to investigate the nonspecific binding of VHH to empty beads. Low ($\Delta Ct < 3$) binding of all the VHHs to the empty beads, indicating that VHH was bound to the gliadin protein and not to the empty beads. Although VHH2 showed a slightly higher ΔCt value with empty beads than the other two VHHs, this was not statistically significant ($p < 0.01$)..

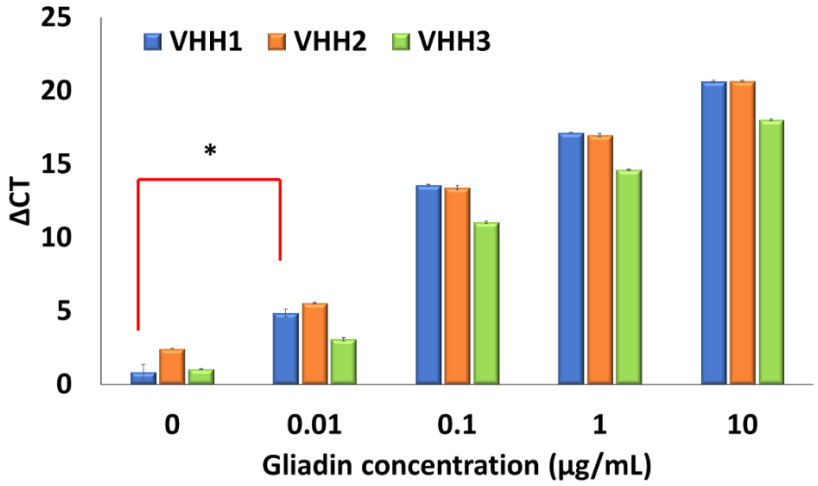

Figure 3.3. Nonspecific binding of VHHs in gliadin-free empty beads. * indicates $p<0.05$, n=3

3.4.2. Specificity confirmation using cD-iPCR

A cD-iPCR experiment was also performed to demonstrate the specificity of a candidate VHH towards gliadin by comparing the affinity with control proteins. VHH1 was used in this experiment because of the higher affinity compared to VHH2 and VHH3. As negative control proteins, anti-GFP VHH (binds to GFP) and BDA (binds to IgG) proteins were used because we already checked their performance in cD-iPCR (Anzai *et al.*, 2019). cDNA display molecules coding VHH1, BDA and anti-GFP VHH were incubated with gliadin beads, IgG beads, GFP beads, or empty beads. Figure 3.4 indicates that the specific binding of VHH1 towards gliadin by giving significantly higher ΔCt value (12.77) which is similar to the control protein anti-GFP VHH (with GFP protein, ΔCt was 14.59). BDA indicated nearly 2-fold increase in binding compared to other two VHH proteins, presumably because of higher cDNA display formation efficiency. Importantly, VHH1 did not show any significant adsorption towards IgG, GFP or empty beads. Also, gliadin protein did not show any stickiness towards control protein BDA or anti-GFP VHH (ΔCt of 4.39 and 2.92, respectively). This control assay demonstrated the specificity of VHH1 for gliadin and gliadin only.

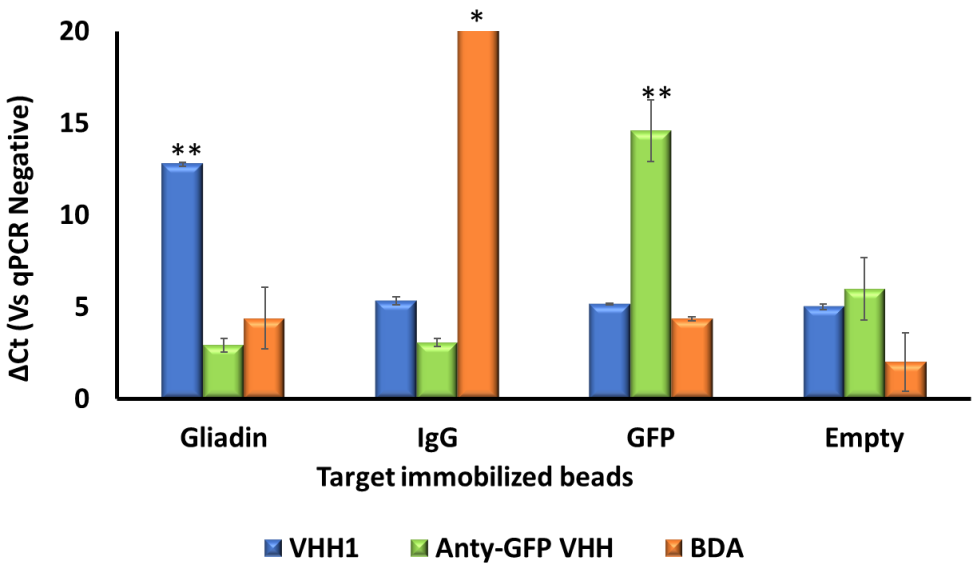

Figure 3.4. The cD-iPCR confirmation of binding specificity and non-specific binding. (VHH1 towards gliadin with control proteins). * indicates p<0.05, ** indicates P<0.001, n=3.

3.4.3. Detection of gliadin in food samples using cD-iPCR

A study was performed to assess whether the VHHs could recognize gliadin in the presence of other food components, using a competitive immunoassay format. Series of gliadin concentrations were spiked into either rice extracts or PBS (control), and cD-iPCR experiments were carried out. As expected, both in rice and buffer, gliadin unspiked samples showed high ΔCt values compared with spiked samples, because there was no loss of VHHs during pre-incubation (Figure 3.5, 0 ng/mL). The data further confirmed that there was no significant difference of ΔCt values in both rice and control buffer samples ($p < 0.01$, *t*-test). This result strongly indicated high specificity of the newly developed VHHs, especially VHH1 and VHH2, as they poorly bound to the rice food matrix. When VHH1 and VHH2 were incubated with 5 ng/mL gliadin (5% gliadin in food), the ΔCt values were significantly ($p < 0.01$, *t*-test) reduced compared with unspiked samples (0%). Also, we observed gradual decrease of ΔCt values between 0 to 5 ng/mL in a concentration-dependent manner.

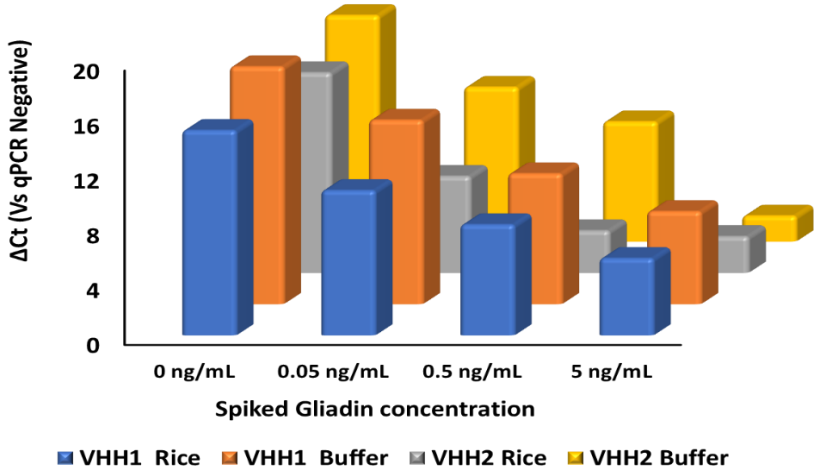

Figure 3.5. Detection of gliadin by VHH1 and VHH2 in the presence and absence of other food matrices. Note: Standard Deviation (SD) is not indicated in the graph and please refer Annex I Table 7 for SD values.

3.4.4. Extraction of gliadin from commercial food samples

Gliadin fractions were extracted from several commercial food samples (not labeled as gluten-free) including control Sigma-Aldrich gliadin from wheat (G3375). The SDS-PAGE profiles revealed the presence of protein bands in standard, breadcrumbs, wheat flour and slightly in oats (~37 KDa). This result showed comparable protein patterns for the Sigma-Aldrich standard gliadin with breadcrumbs and wheat flour, although in the latter, the band intensities are lower, while the other food samples (rice crackers, potato starch and corn flour) has no gliadins (Figure 3.6).

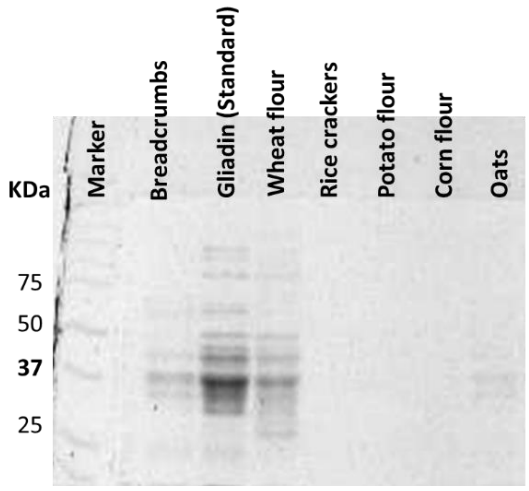

Figure 3.6. SDS-PAGE analysis of Gliadin extraction. Standard (2 mg/mL) and other food samples (20mg/mL).

3.4.5. Detection of gliadin in commercial food samples using cD-iPCR

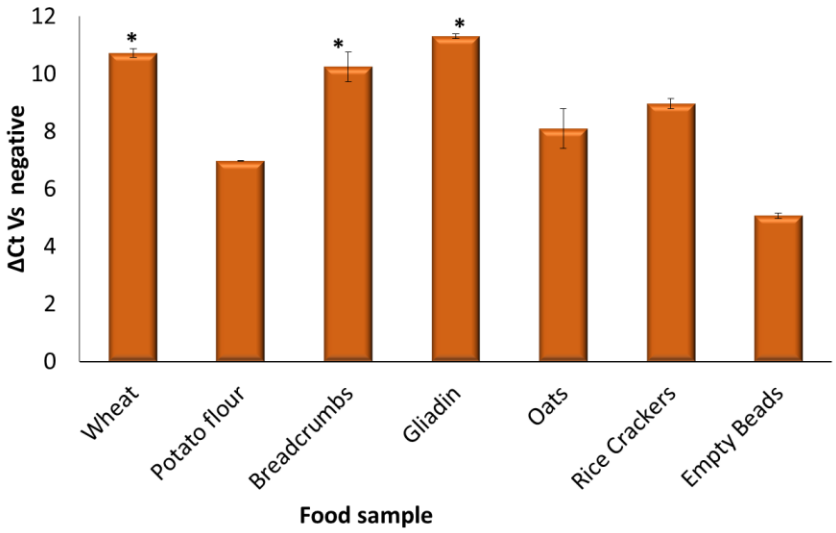

Figure 3.7. Gliadin detection in commercial food extracts with cD-iPCR

Finally, a study was performed to recognize the presence of gliadin commercial food components, using cD-iPCR. Gliadin extracts of food samples were immobilized on C-4 magnetic beads, and the cD-iPCR experiments were carried out with equal amounts of VHH1 cDNA display molecules.

As expected, food samples which contain gliadin (standard gliadin, wheat flour, breadcrumbs) showed high ΔCt values compared with samples which do not contain gliadin (potato starch, rice crackers and oats). Although the standard gliadin showed strong presence in the extract on SDS-PAGE analysis (Figure 3.7), the cD-iPCR results do not indicate significant increase in ΔCt value compared with wheat flour and breadcrumbs. Moreover, potato starch, rice crackers and oats also showed considerable ΔCt values even though they do not contain gliadin naturally. This may be due to the high non-specific binding of magnetic beads as empty beads also showed reasonably high ΔCt value.

3.5. Conclusions

In conclusion, the novel PCR-based antigen detection method (cD-iPCR), which takes an advantage of the structural characteristics of cDNA display (a peptide-cDNA conjugate developed for in vitro evolution of polypeptides), proved to work in detecting affinity sensitivities of naively developed VHHs against gliadin protein and the data were comparable with ELISA and pull-down assays. When considering the gliadin detection in commercially available food samples, VHH1 tend to recognize gliadin in food samples however non-specific binding seems to be a huge obstacle in practical applications.

Chapter 4

Overall discussion and conclusion

4.1. Discussion

Gliadin is the storage protein in wheat grain that is soluble in aqueous alcohols but is insoluble in water or neutral salt solutions. In general, gliadin is extracted with aqueous alcohol (60%–70%) (Chu and Wen, 2013; Urade, Sato and Sugiyama, 2018; Altenbach *et al.*, 2019). In the present study, gliadin was extracted with 70% alcohol (with or without 10% DMSO) in PBS buffer. Insolubility in aqueous solutions/ buffers and incomplete extraction of the protein were some of the obstacles in the process of immobilizing gliadin on magnetic beads. Since gliadin is a complex mixture of proteins, it was also challenging to immobilize gliadin completely and evenly on the beads during each selection round (Miranda-Castro *et al.*, 2016). , Gliadin proteins are divided into subgroups of α-, γ-, β- and ω-gliadins. The group of α- gliadins is generally the major group, comprising between 44% and 60% of the total gliadin content. The second largest group is γ-gliadins (31%–46%), and together these groups account for about 80% of wheat gliadins (Shewry and Tatham 1990). The α- and γ- gliadins are often combined and simply referred to as α- gliadins because of the high similarity of their N-terminal amino acid sequences. After considering several bead immobilization methods, the antigenic gliadin proteins were covalently coupled to NHS-activated carboxylic acid beads to achieve maximum immobilization. This method allowed approximately 60%-70% immobilization of medium-molecular weight gliadin groups only on the beads.

The cDNA display method is an immunization-free *in vitro* selection tool which is important when comes to obtaining antibodies that can recognize targets which cannot be used in immunizing

animals due to their low immunogenicity or toxicity. The present study aimed to select VHH antibodies against wheat gliadin from an alpaca derived naïve VHH library. Since gliadin is not immunogenetic in all animals, it is difficult to ensure the formation of suitable antibodies by immunization techniques. Besides, some studies have indicated that the immunological response to antigen vaccines in children, even those with CD, does not differ markedly from that of the general population (Anania *et al.*, 2017). Hence, *in vitro* selection techniques may be necessary for screening antibodies against variable toxins, such as gliadin. The key feature of the cDNA display method is the easy to use preparation using a unique puromycin linker, which is hybridized and photo-ligated to the 3'-end of mRNA (Yamaguchi *et al.*, 2009; Mochizuki *et al.*, 2015; Eden *et al.*, 2017). The method proved to screen many affinity peptides/VHHs successfully without using experimental animals. The cDNA display enables the successful selection of high-affinity VHH from synthetic libraries, with a library size of over 10^{13}. This method has several characteristics that assist in improving many drawbacks (e.g. instability, limited diversity or small library size, cell toxicity of proteins, effect of fused coat proteins, and difficult handling) that are occur either cell dependent (i.e., phage display, bacterial display, yeast display) or cell-independent (i.e., ribosome display, mRNA display) in vitro selection techniques. The successful formation and purification of cDNA display molecules was confirmed by SDS-PAGE. Although the formation yield of the cDNA display molecules seems to be low (5.6%), it was in line with our previous studies, in which the formation efficiency of the cDNA display for small polypeptides was observed to be approximately 5%–25% (Yamaguchi *et al.*, 2009; Biyani *et al.*, 2011; Mochizuki *et al.*, 2011). However, it is important to improve the formation efficiency of the cDNA display molecule and we are currently working on this issue. Here, *in vitro* affinity selection was performed using constructed VHH-coding cDNA display molecules toward immobilized gliadin,

and three candidate VHHs were successfully selected. When the number of selections was increased the elute quantity was also increased and reached a plateau, indicating enrichment of the binders. The band intensities of the last selection round were graphically compared with the parallel negative selection band intensities. The intensity of the positive selection elution band was considerably higher (by approximately 11-fold) than the negative selection elution band. This result indicated high specific and low nonspecific binging of candidate VHHs. Following the in vitro selection, all the selection elutes were analyzed by NGS, instead of analyzing the last selection elute only, to generate more comparable sequence data. According to the percentage abundance (frequency) of the NGS data, the top three VHH sequences, which were not appeared in the negative selection data pool were selected as candidate VHH sequences. Dona *et al*., describes that single domain antibodies are especially suitable for quantitative determination of gliadins under denaturing conditions. Further, ethanol and denaturing agents used in prolamin extraction interfere with antigen recognition by conventional antibodies. The study explained that VHH antibodies can detect gliadins in samples shown as negatives by conventional ELISA resulting in dissociation constants next to the 10^{-7} M range. Therefore, usage of VHH antibody appears as an excellent platform for quantitative determination of proteins or any other immunogenic compound, in the presence of denaturing agents, when specific recognition units with high stability are required (Dona *et al*., 2010).

Determination of the interactions between the selected VHHs and the target gliadin is an essential step toward understanding the affinity. In the pulldown assay, specificity of the anti-gliadin VHH towards gliadin were confirmed by comparing with control proteins including a single chain peptide (BDA) and a single domain antibody (anti-GFP VHH). The results confirmed that VHH1 is specifically bound with gliadin and gliadin only, and the observed binding was not from potential

stickiness to the gliadin. In the study, data (not mentioned in the text) indicated that anti-gliadin VHH appeared to recognize several toxic protein components of the target gliadin. Gliadin is a large family of proteins with closely similar amino acid sequences, but different molecular weights. These proteins have been classified as α, β, γ, and ω gliadins (Urade, Sato and Sugiyama, 2018; Altenbach *et al.*, 2019). This multiple protein binding is important because the developed VHHs may be able to recognize almost all the toxic gliadin components present in food. Similar result was observed in several other anti-gluten antibodies developed to date (Panda *et al.*, 2015; Kanerva *et al.*, 2011). The differences in the CDR regions are likely to be responsible for this multiple binding, but further studies are required for confirmation. In ELISA assay, results indicated increasing binding of VHH at higher concentrations. Also, higher detection signals were observed for VHH1 and VHH2 candidates compared to VHH3, which was comparable with the pulldown assay and cD-iPCR assay results. Moreover, data indicated the non-specific binding of anti-gliadin VHH to BSA protein was considerably low and at the same time there was no association of anti-BSA VHH to gliadin. However, in ELISA was not able to show any saturated signal even when the concentration reached to 10 µg/mL.

As a novel immuno-qPCR application, we applied our previously developed cD-iPCR assay successfully in this study to understand the binding patterns and specificity of selected VHHs towards gliadin. Compared with other immuno-PCR methods, the cD-iPCR method is unique because of the covalent conjugation mechanism. In this method, the peptide is always conjugated covalently to DNA at a ratio of 1:1 (Anzai *et al.*, 2019). Because of the sensitivity of the assay, binding of the VHH to very low gliadin concentrations (i.e., 0.001 µg/mL) was able to be detected with a statistical significance ($p < 0.01$, *t*-test). VHH1 and VHH2 were the best binders according to the immuno-PCR assay and the results were similar to the results of other assays. In the

specificity confirmation assay for the VHH1 against two other control proteins (BDA and anti-GFP VHH), the data indicated that VHH1 is uniquely bound to gliadin protein. The data was in line with the results observed in pulldown assay. A preliminary study was performed to assess the applicability of the developed VHHs in detecting gliadin in food to determine whether VHHs can recognize gliadin in the presence of other food components. The cD-iPCR method was used as a competitive immunoassay, and the data indicated a positive detection pattern with increasing gliadin concentrations. When the amount of spiked gliadin reached 5% of the food sample (5 ng/ mL spiked gliadin in 100 ng/mL rice), the detection was statistically significant ($p < 0.01$). However, the ΔCt values of lower spiked concentrations (0.5% and 0.05%) were not significant enough and further optimization is necessary to improve sensitivity. Food extracts contain a mixture of compounds, which can act as nonspecific binders with the detector antibodies (Cucu *et al.*, 2012; Koppelman *et al.*, 2015). Hence, it is a critical and difficult task to perform detection assays in actual food. As discussed here, these cDNA display-based assays will open new avenues for gluten quantification. Nevertheless, we believe that the cD-iPCR method can be applied with even higher sensitivity levels after making improvements to the binders. Although still in its infancy, we believe that gliadin detection using selected VHHs will undoubtedly continue to advance.

4.2. Conclusions

A naïve VHH DNA library was used successfully for selecting VHH candidates that specifically bound to toxic gliadin, without immunizing animals, using the cDNA display assay. The presence of several components in the gliadin protein mixture was a challenge as this might cause uneven immobilization of the protein on the beads during each selection round. Three candidate VHHs were selected at the end of the in vitro selection. The cD-iPCR method was used to identify the affinity interactions successfully and the data were comparable with ELISA and pull-down assays. VHH1 and VHH2 were the best binders toward gliadin compared with VHH3 in all assays performed, including the cD-iPCR assay. Even though the candidate VHH1 and VHH2 showed considerable affinities toward gliadin, more investigation and optimization are required before they can be used in practical applications. VHH1 tend to recognize gliadin in food samples however non-specific binding seems to be a huge obstacle in practical applications. We believe, this study opens new paths to combine advanced technologies, such as the cDNA display method and cD-iPCR, to obtain effective binders for toxic and complex proteins, which is difficult to achieve using conventional methods. Also, these immunization-free affinity antibody preparation technologies may reach the ethics and principles of modern scientific experimentation, especially in terms of animal protection.

Acknowledgement

Firstly, I would like to express my sincere gratitude to my supervisor, Professor Naoto Nemoto for the continuous support of my Ph.D. study and related research, for his patience, motivation, and immense knowledge. His guidance helped me in all the time of research and writing of this thesis. I could not have imagined having a better advisor and mentor for my Ph.D. study. I am truly and sincerely thankful for his constant readiness during this whole pursuit, to listen and to provide fresh impulse in acquiring the skill of independent scientific research.

Concomitantly, my sincere thank goes to the research evaluation committee: Professor Miho Suzuki, Professor Yuzuru Tozawa and Professor Koji Matsuoka for their guidance and support throughout the study effort.

I am thankful to Dr. Takuya Terai for the countless scientific discussions which I always learnt something new.

Besides, I am very much thankful to Ms. Akiko Ishiguro for her ceaseless facilitation and goodwill in all the laboratory affaires. I would also like to thank all my lab mates for their heartening and consoling during my spell in Saitama University as I value it for the lifetime.

I greatly appreciate the support received through the collaborative work undertaken with the Epsilon Molecular Engineering (EME) Inc., during the first phase of my research work.

Ultimately, I express my profound gratitude to my family for providing me with unfailing support and continuous encouragement throughout my years of study.

References

Altenbach SB, Chang HC, Yu XB, Seabourn BW, Green PH, Alaedini A (2019) Elimination of Omega-1,2 Gliadins from Bread Wheat (Triticum aestivum) Flour: Effects on Immunogenic Potential and End-Use Quality, Frontiers in Plant Science. 10(580).

Al-Toma A, Volta U, Auricchio R, Castillejo G, Sanders D, Cellier C, Mulder CJ, Lundin KAE. (2019) European Society for the Study of Coeliac Disease (ESsCD) guideline for coeliac disease and other gluten-related disorders. United European Gastroenterol J. 7(5):583-613.

Anania C, Olivero F, Spagnolo A, Chiesa C, Pacifico L. (2017) Immune response to vaccines in children with celiac disease. World J Gastroenterology. 23(18):3205–3213.

Anzai H, Terai T, Jayathilake C, Suzuki T, Nemoto N. (2019) A novel immuno-PCR method using cDNA display. Analytical Biochemistry. 1(578):1–6.

Arnold FH, Volkov AA. (1999) Directed evolution of biocatalysts, Current opinion in chemical biology. 3(1):54–9.

Balakireva, AV, Zamyatnin, AA. (2016) Properties of Gluten Intolerance: Gluten Structure, Evolution, Pathogenicity and Detoxification Capabilities. Nutrients. 8(10):e644.

Barendt PA, Ng DT, McQuade CN, Sarkar CA. (2013) Streamlined protocol for mRNA display. ACS Combinatorial Science. 15(2):77–81.

Barton SH, Murray JA. (2008) Celiac disease and autoimmunity in the gut and elsewhere. Gastroenterology Clinics of North America. 37(2):411–vii.

Biesiekierski JR., Peters SL, Newnham ED, Rosella O, Muir JG, Gibson PR. (2013) No effects of gluten in patients with self-reported non-celiac gluten sensitivity after dietary reduction of fermentable, poorly absorbed, short-chain carbohydrates. Gastroenterology. 145(2):320–328.

Biyani M, Biyani M, Nemoto N, Ichiki T, Nishigaki K, Husimi Y. (2011) Gel shift selection of translation enhancer sequences using messenger RNA display. Analytical Biochemistry. 409(1):105–111.

Boder, ET, Midelfort, KS, Wittrup, KD. (2000) Directed evolution of antibody fragments with monovalent femtomolar antigen-binding affinity. Proceedings of the National Academy of Sciences of the United States of America. National Academy of Sciences, 97(20):10701–10705.

Carroccio A, Mansueto P, Iacono G, Soresi M, D'Alcamo A, Cavataio F, Brusca I, Florena AM, Ambrosiano G, Seidita A, Pirrone G, Rini GB. (2012) Non-celiac wheat sensitivity diagnosed by double-blind placebo-controlled challenge: exploring a new clinical entity. American J of Gastroenterology 107(12):1898–1906.

Casella G, Villanacci V, Di Bella C, Bassotti G, Bold J, Rostami K. (2018) Non celiac gluten sensitivity and diagnostic challenges. Gastroenterol Hepatol Bed Bench. 11(3):197–202.

Catassi C, Elli L, Bonaz B, Bouma G, Carroccio A, Castillejo G., … Fasano A. (2015). Diagnosis of Non-Celiac Gluten Sensitivity (NCGS): The Salerno Experts' Criteria. Nutrients, 7(6):4966–4977.

Chu PT, Wen HW. (2013) Sensitive detection and quantification of gliadin contamination in gluten-free food with immunomagnetic beads based liposomal fluorescence immunoassay. Analytica Chimica Acta. 17(787):246–253.

Cucu T, Devreese B, Trashin S, Kerkaert B, Rogge M, De Meulenaer B. (2012) Detection of hazelnut in foods using ELISA: challenges related to the detectability in processed foodstuffs. J of AOAC International, 95(1):149–56.

Czaja-Bulsa G, Bulsa M. (2017) What Do We Know Now about IgE-Mediated Wheat Allergy in Children? Nutrients. 9(1):35.

De Vlieger D, Ballegeer M, Rossey, Schepens B, Saelens X. (2018) Single-Domain Antibodies and Their Formatting to Combat Viral Infections. Antibodies. 8(1):E1.

Desmyter A, Transue TR, Ghahroudi MA, Thi MH, Poortmans F, Hamers R, Muyldermans S, Wyns L. (1996) Crystal structure of a camel single-domain VH antibody fragment in complex with lysozyme. Nature Structural Biology. 3:803–811.

Dewar D, Pereira SP, Ciclitira PJ. (2004) The pathogenesis of coeliac disease. The International J of Biochemistry & Cell Biology. 36(1):17–24.

Doña V, Urrutia M, Bayardo M, Alzogaray V, Goldbaum FA, Chirdo FG. (2010) Single domain antibodies are specially suited for quantitative determination of gliadins under denaturing conditions. Journal of Agriculture and Food Chemistry. 58(2):918-26.

Eden T, Menzel S, Wesolowski J, Bergmann P, Nissen M, Dubberke G, Seyfried F, Albrecht B, Haag F, Koch-Nolte F. (2017) A cDNA Immunization Strategy to Generate Nanobodies against Membrane Proteins in Native Conformation. Frontiers in immunology. 8:1989.

Fasano A, Catassi C. (2012) Clinical practice. Celiac disease. The New England J of Medicine. 367(25):2419–2426.

Fasano, A. Catassi, C. (2001) Current approaches to diagnosis and treatment of celiac disease: An evolving spectrum. Gastroenterology. 120(3):636–651.

Fields S, Song OK. (1989) A novel genetic system to detect protein-protein interactions. Nature, 340(6230):245–246.

Gai SA, Wittrup KD. (2007) Yeast surface display for protein engineering and characterization. Current Opinion in Structural Biology. 17(4):467–473.

Geisslitz S, Wieser H, Scherf KA, Koehler P. (2018) Gluten protein composition and aggregation properties as predictors for bread volume of common wheat, spelt, durum wheat, emmer and einkorn. J of Cereal Science. 83:204–212.

Gold L., Allen,P., Binkley,J., Brown,D., Schneider,D., Eddy,S.R., Tuerk,C., Green,L., MacDougal,S. and Tasset,D. (1993) In Gesteland,R.R. and Atkins,J.F. (eds), The RNA world. Cold Spring Harbor Laboratory, Cold Spring Harbor, NY, pp. 497–509.

Gonzalez-Sapienza G, Rossotti MA, Tabares-da Rosa S. (2017) Single-Domain Antibodies as Versatile Affinity Reagents for Analytical and Diagnostic Applications. Frontiers in Immunology. 8:977.

Green PH, Cellier C. (2007) Celiac disease. The New England J of Medicine. 357(17):1731-43.

Guo YC, Zhou YF, Zhang XE, Zhang ZP, Qiao YM, Bi LJ, Wen JK, Liang MF, Zhang JB. (2006) Phage display mediated immuno-PCR. Nucleic Acids Research. 34(8):e62.

Hamers-Casterman C, Atarhouch T, Muyldermans S, Robinson G, Hamers C, Songa EB, Bendahman N & Hamers R. (1993) Naturally occurring antibodies devoid of light chains. Nature. 363(6428): 446-448.

Hanes J, Pluckthun A. (1997) In vitro selection and evolution of functional proteins by using ribosome display. Proceedings of the National Academy of Sciences, 94(10):4937–4942.

Hendrickson, E. R., Truby, T. M., Joerger, R. D., Majarian, W. R. and Ebersole, R. C. (1995). High sensitivity multianalyte immunoassay using covalent DNA-labeled antibodies and polymerase chain reaction. Nucleic Acids Res 23(3): 522-529.

Holliger P, Hudson PJ. (2005) Engineered antibody fragments and the rise of single domains. Nature Biotechnology. 23(9):1126–1136.

Husby S, Koletzko S, Korponay-Szabo IR, Mearin ML, Phillips A, Shamir R, Troncone R, Giersiepen K, Branski D, Catassi C et al. (2012) European Society for Pediatric Gastroenterology, Hepatology, and Nutrition guidelines for the diagnosis of coeliac disease. J. of Pediatric Gastroenterology and Nutrition. 54(1):136–160.

Husby S, Murray JA, Katzka DA. (2019) AGA Clinical Practice Update on Diagnosis and Monitoring of Celiac Disease—Changing Utility of Serology and Histologic Measures: Expert Review. Gastroenterology. 156(4):885–889.

Inna Spector Cohen M.D, Andrew S. Day M.D, Ron Shaoul MD. (2019) Gluten in Celiac Disease-More or Less? Rambam Maimonides Medical J, 10(1):e0007.

Jiang X, Cheng S, Chen W, Wang L, Shi F, Zhu C. (2012) Comparison of oligonucleotide-labeled antibody probe assays for prostate-specific antigen detection. Analytical Biochemistry. 424(1):1-7.

Kanerva P, Sontag-Strohm T, Brinck O. (2011) Improved extraction of prolamins for gluten detection in processed foods. Agricultural and Food Science. 20(3):206-216.

Koch-Nolte F, Reyelt J, Schössow B, Schwarz N, Scheuplein F, Rothenburg S, Haag F, Alzogaray V, Cauerhff A, Goldbaum FA (2007) Single domain antibodies from llama effectively and specifically block T cell ecto-ADP-ribosyltransferase ART2.2 in vivo. FASEB J. 21(13):3490–3498.

Koppelman SJ, Söylemez G, Niemann L, Gaskin FE, Baumert JL, Taylor SL. (2015) Sandwich Enzyme-Linked Immunosorbent Assay for Detecting Sesame Seed in Foods. BioMed research international. 2015:853836-16.

Leffler DA, Green PH, Fasano A. (2015) Extraintestinal manifestations of coeliac disease. Nature Reviews Gastroenterology & Hepatology. 12(10):561–571.

Lim SD, Min H, Youn E, Kawasaki I, Shim Y. (2018). Gliadin intake induces oxidative-stress responses in Caenorhabditis elegans. Biochemical and biophysical research communications. 503(3):2139-2145.

Lionetti, E. Castellaneta S, Francavilla R, Pulvirenti A, Catassi GN, Catassi C. (2019) Long-Term Outcome of Potential Celiac Disease in Genetically At-Risk Children: The Prospective CELIPREV Cohort Study. Journal of Clinical Medicine. 8(2):186.

Lipovsek D, Plückthun A. (2004) In-vitro protein evolution by ribosome display and mRNA display. J. Immunology. Met. 290(1-2)51-67.

Longo G, Berti I, Burks AW, Krauss B, Brabie E. (2013) IgE-mediated food allergy in children. The Lancet. 382(9905):1656–1664.

Luo XM, McKeague M, Pitre S, Dumontier M, Green J, Golshani A, Derosa MC, Dehne F (2010) Computational approaches toward the design of pools for the in vitro selection of complex aptamers. Rna-a Publication of the Rna Society. 16(11): 2252-2262.

Manai F, Azzalin A, Gabriele F, Martinelli C, Morandi M, Biggiogera M, Bozzola M, Comincini S. (2018) The In Vitro Effects of Enzymatic Digested Gliadin on the Functionality of the Autophagy Process. International journal of molecular sciences. 19(2):E635.

Marshall KA, Ellington AD. (2000) In vitro selection of RNA aptamers. Methods in Enzymology. 318:193-214.

Miranda-Castro R, de-los-Santos-Álvarez N, Miranda-Ordieres AJ, Lobo-Castañón MJ. (2016) Harnessing Aptamers to Overcome Challenges in Gluten Detection. Biosensors (Basel). 6(2):16.

Mochizuki Y, Biyani M, Tsuji-Ueno S, Suzuki M, Nishigaki K, Husimi Y, Nemoto N. (2011) One-Pot Preparation of mRNA/cDNA Display by a Novel and Versatile Puromycin-Linker DNA. ACS Combinatorial Science. 13(5):478–485.

Mochizuki Y, Suzuki T, Fujimoto K, Nemoto N. (2015) A versatile puromycin-linker using cnvK for high-throughput in vitro selection by cDNA display. Journal of Biotechnology. 212:174–180.

Moutel S, Bery N, Bernard V, Keller L, Lemesre E, de Marco A, Ligat L, Rain JC, Favre G, Olichon A, Perez F. (2016) NaLi-H1: A universal synthetic library of humanized nanobodies providing highly functional antibodies and intrabodies. ELife, 5:e16228.

Muyldermans S, Cambillau C, Wyns L. (2001) Recognition of antigens by single-domain antibody fragments: the superfluous luxury of paired domains. Trends Biochemical Science. 26(4):230–235.

Nemoto N, Fukushima T, Kumachi S, Suzuki M, Nishigaki K, Kubo T. (2014) Versatile C-Terminal Specific Biotinylation of Proteins Using Both a Puromycin-Linker and a Cell-Free Translation System for Studying High-Throughput Protein–Molecule Interactions. Analytical Chemistry. 86(17):8535–8540.

Nemoto N, Miyamoto-Sato E, Husimi Y, Yanagawa H. (1997) In vitro virus: bonding of mRNA bearing puromycin at the 3'-terminal end to the C-terminal end of its encoded protein on the ribosome in vitro. FEBS Letters. 414(2):405-8.

Nguyen VK, Su C, Muyldermans S, van der Loo W. (2002) Heavy-chain antibodies in Camelidae; a case of evolutionary innovation. Immunogenetics. 54(1):39–47.

Nilsen EM, Jahnsen FL, Lundin KE, Johansen FE, Fausa O, Sollid LM, Jahnsen J, Scott H, Brandtzaeg P. (1998) Gluten induces an intestinal cytokine response strongly dominated by interferon gamma in patients with celiac disease. Gastroenterology. 115(3):551–563.

Olichon A, de Marco A. (2012) Preparation of a Naïve Library of Camelid Single Domain Antibodies. Methods in Molecular Biology. 911:65–78.

Ontiveros N, Rodríguez-Bellegarrigue CI, Galicia-Rodríguez G, Vergara-Jiménez MJ, Zepeda-Gómez EM, Arámburo-Galvez JG, Gracia-Valenzuela MH, Cabrera-Chávez F. (2018) Prevalence of Self-Reported Gluten-Related Disorders and Adherence to a Gluten-Free Diet in Salvadoran Adult Population. International journal of environmental research and public health. 15(4):E786.

Osborne T.B (1907) The Proteins of the Wheat Kernel. Washington DC: Carnegie Institute of Washington, doi.org/10.5962/bhl.title.22763.

Palosuo K, Varjonen E, Kekki OM, Klemola T, Kalkkinen N, Alenius H, Reunala T. (2001) Wheat ω-5 gliadin is a major allergen in children with immediate allergy to ingested wheat. J Allergy and Clinical Immunology. 108(4):634-638.

Panda R, Zoerb HF, Cho CY, Jackson LS, Garber EA. (2015) Detection and Quantification of Gluten during the Brewing and Fermentation of Beer Using Antibody-Based Technologies. 78(6):1167-77.

Parzanese I, Qehajaj D, Patrinicola F, Aralica M, Chiriva-Internati M, Stifter S, Elli L, Grizzi F. (2017) Celiac disease: From pathophysiology to treatment. World J Gastrointestinal Pathophysiology. 8(2):27-38.

Perez JW, Vargis EA, Russ PK, Haselton FR, Wright DW. (2011) Detection of respiratory syncytial virus using nanoparticle amplified immuno-polymerase chain reaction, Analytical Biochemistry. 410 (1):141-148.

Rasheed A, Xia X, Yan Y, Apples R, Mahmood T, He Z. (2014) Wheat seed storage proteins: Advances in molecular genetics, diversity and breeding applications. Journal of Cereal Science. 60(1):11–24.

Roberts RW. (1999) Totally in vitro protein selection using mRNA-protein fusions and ribosome display. Current Opinion in Chemical Biology. 3(3):268-273.

Sabir JS, Atef A, El-Domyati FM, Edris S, Hajrah N, Alzohairy AM, Bahieldin A. (2014) Construction of naïve camelids VHH repertoire in phage display-based library. Comptes Rendus Biologies, 337(4):244–249.

Saeed A, Assiri A, Cheema H. (2019) Celiac disease in children. J of Nature and Science of Medicine. 2(1):23.

Salvador JP, Vilaplana L, Marco MP. (2019) Nanobody: outstanding features for diagnostic and therapeutic applications. Analytical and Bioanalytical Chemistry. 411(9):1703–1713.

Sano T, Smith C, Cantor C. (1992) Immuno-PCR: very sensitive antigen detection by means of specific antibody-DNA conjugates. Science. 258(5079):120–122.

Sapone A, Bai J, Ciacci C, Dolinsek J, Green PH, Hadjivassiliou M, Kaukinen K, Rostami K, Sanders DS, Schumann M, et al. (2012) Spectrum of gluten disorders: Consensus on new nomenclature and classification. BMC Medicine. 10(13).

Schaffitzel C, Hanes J, Jermutus L, Plückthun A. (1999) Ribosome display: an in vitro method for selection and evolution of antibodies from libraries. Journal of Immunological Methods. 231(1-2):119–135.

Scherf KA, Koehler P, Wieser H. (2016) Gluten and wheat sensitivities – An overview. Journal of Cereal Science. 67:2–11.

Scheuplein F, Rissiek B, Driver JP, Chen Y-G, Koch-Nolte F & Serreze DV (2010) A recombinant heavy chain antibody approach blocks ART2 mediated deletion of an iNKT cell population that upon activation inhibits autoimmune diabetes. J. Autoimmunology. 34(2):145–154.

Schuppan D. (2000) Current concepts of celiac disease pathogenesis. Gastroenterology. 119(1):234–242.

Shan L, Molberg Ø, Parrot I, Hausch F, Filiz F, Gray GM, Sollid LM, Khosla C. (2002) Structural basis for gluten intolerance in Celiac Sprue. Science. 297(5590):2275–2279.

Shewry PR, Brennan C, Tatham AS, Warburton T, Fido R, Smith D, Griggs D, Cantrell I, Harris N. (1996) The development, structure and composition of the barley grain in relation to its end use properties. In: Cereals 96. Proceedings of the 46th Australian Cereal Chemistry Conference, Sydney, 158–162.

Shewry PR, Popineau Y, Lafiandra D, Belton P. (2000) Wheat glutenin subunits and dough elasticity: findings of the EUROWHEAT project. Trends in Food Science & Technology. 11(12):433–441.

Shewry PR, Tatham AS, Barro F, Barcelo P, Lazzeri P. (1995) Biotechnology of breadmaking: unravelling and manipulating the multi-protein gluten complex. Nature Biotechnology. 13:1185–1190.

Shewry PR, Tatham AS, Halford NG. (1999) The prolamins of the Triticeae. In: Shewry PR, Casey R, eds. Seed proteins. Dordrecht: Kluwer Academic Publishers, 35–78.

Shewry PR, Tatham AS. (1990) The prolamin storage proteins of cereal seeds: structure and evolution. Biochemical J. 267(1):1-12.

Shewry PR, Tatham AS. (1997) Disulphide bonds in wheat gluten proteins. J Cereal Science. 25(3):207-227.

Shewry PR, Tatham AS. (1999) The characteristics, structures and evolutionary relationships of prolamins. In: Seed proteins. Shewry P.R. and Casey R. (Eds.). Kluwer Academic Publishers, the Netherlands. pp. 11-34.

Shewry PR. (1999) The synthesis, processing and deposition of gluten proteins in the developing wheat grain. Cereal Foods World. 44, 587–589.

Skerritt JH. (1985) A sensitive monoclonal-antibody-based test for gluten detection: quantitative immunoassay. J of the Science of Food and Agriculture. 36(10):987-994.

Smith GP, Petrenko VA. (1997) Phage Display. Chemical Reviews. 97(2):391–410.

Stahl S, Uhlen M. (1997) Bacterial surface display: trends and progress. Trends in Biotecnology. 1997, 15(5):185-192.

Suzuki T, Mochizuki Y, Kimura S, Akazawa-Ogawa Y, Hagihara Y, Nemoto N. (2018) Anti-survivin single-domain antibodies derived from an artificial library including three synthetic random regions by in vitro selection using cDNA display. Biochemical and Biophysical Research Communications. 503(3):2054–2060.

Tanemura Y, Mochizuki Y, Kumachi S, Nemoto N. (2015) Easy and rapid binding assay for functional analysis of disulfide-containing peptides by a pull-down method using a puromycin-linker and a cell-free translation system. Biology. 4(1):161–72.

Tawfik DS, Griffiths AD. (1998) Man-made cell-like compartments for molecular evolution. Nature Biotechnology. 16(7):652–656.

Terai T, Anzai H, Nemoto N. (2019) Selection of Peptides that Associate with Dye-Conjugated Solid Surfaces in a pH-Dependent Manner Using cDNA Display. ACS Omega. 4(4):7378-7384.

Tijink BM, Laeremans T, Budde M, Stigter-van Walsum M, Dreier T, de Haard HJ, Leemans CR, van Dongen GAMS (2008) Improved tumor targeting of anti-epidermal growth factor receptor Nanobodies through albumin binding: taking advantage of modular Nanobody technology. Molecular Cancer Therapeutics. 7(8):2288–2297.

Ueno S, Nemoto, N. (2012) CDNA display: Rapid stabilization of mRNA display. Methods in Molecular Biology. 805:113–135.

Ullman CG, Frigotto L, Cooley RN. (2011) In vitro methods for peptide display and their applications. Briefings in Functional Genomics. 10(3):125–134.

Urade R, Sato N, Sugiyama M. (2018) Gliadins from wheat grain: an overview, from primary structure to nanostructures of aggregates. Biophysical reviews. 10(2):435–443.

van Buggenum, J. A. G. L., Gerlach, J. P., Eising, S., Schoonen, L., van Eijl, R. A. P. M., Tanis, S. E. J., Hogeweg, M., Hubner, N. C., van Hest, J. C., Bonger, K. M. and Mulder, K. W. (2016). A covalent and cleavable antibody-DNA conjugation strategy for sensitive protein detection via immuno-PCR. Sci. Rep 6, 22675.

Van Heel DA, West J. (2006) Recent advances in coeliac disease. Gut. 55(7):1037–1046.

Vu KB, Ghahroudi MA, Wyns L & Muyldermans S (1997) Comparison of llama VH sequences from conventional and heavy chain antibodies. Molecular Immunology. 34(16-17): 1121–1131.

Wesolowski J, Alzogaray V, Reyelt J, Unger M, Juarez K, Urrutia M, Cauerhff A, Danquah W, Rissiek B, Scheuplein F, Schwarz N, Boyer O, Seman M, Licea A, Serreze DV, Goldbaum FA, Haag F, Koch-Nolte F. (2009) Single domain antibodies: promising experimental and therapeutic tools in infection and immunity. Medical Microbiology and Immunology. 198(3): 157–174.

Yamaguchi J, Naimuddin M, Biyani M, Sasaki T, Machida M, Kubo T, Funatsu T, Husimi Y, Nemoto N. (2009) cDNA display: a novel screening method for functional disulfide-rich peptides by solid-phase synthesis and stabilization of mRNA-protein fusions. Nucleic Acids Research. 37(16):e108.

Yano H. (2019) Recent practical researches in the development of gluten-free breads. Science of Food. 3(1):7.

Zahnd C, Amstutz P, Plückthun A. (2007) Ribosome display: selecting and evolving proteins in vitro that specifically bind to a target. Nature Methods. 4(3):269-79.

Annex I

Table 1. Reaction buffers compositions.

1x PBS	137 mM Sodium Chloride, 10 mM phosphate, 2.7 mM Potassium Chloride, pH 7.4
Gliadin immobilization buffer	PBS buffer, 70% ethanol, 10% DMSO
Binding buffer	20 mM Tris-HCl, 2 mM EDTA, 2 M NaCl, 0.2% (v/v) Tween 20, pH 7.4
His tag binding buffer	20 mM sodium phosphate buffer, 0.5 M NaCl, 5 mM imidazole, pH 7.4
His tag wash buffer	20 mM sodium phosphate buffer, 0.5 M NaCl, 20 mM imidazole, pH 7.4
His tag elution buffer	20 µL, 20 mM sodium phosphate buffer, 0.5 M NaCl, 250 mM imidazole, pH 7.4
SDS/DTT elution buffer	1% (v/v) SDS, 50 mM DTT, 50 mM Tris-HCl, 0.5 M NaCl, 1mM EDTA, 0.05% (v./v) Tween 20, pH 7.4

Table 2. Sequences of the DNA fragments used in constructing VHH DNA.

Fragment name	**sequence（5' to 3'）**
T7 promoter, omega (Ω) enhancer, Kozak consensus sequence	GATCCCGCGAAATTAATACGACTCACTATAGGGGAAGTAT TTTTACAACAATTACCAACAACAACAACAAACAACAACA ACATTACATTTTACATTCTACAACTACAAGCCACCATG
His-tag, and linker	GGGGGAGGCAGCCATCATCATCATCATCACGGCGGAAGC

hybridization (LHR)	region	AGGACGGGGGGCGGCGTGGAAA

Table 3. Primers used in the study.

Primer name	**sequence（5' to 3'）**
Alp-Sfi-VHH-F1	CTGCTCCTCGCGGCCCAGCCGGCCATGGCTSAGKTGCAG CTCGTGGAGTC
Alp-Sfi-SHinge-R	TTTGCTCTGCGGCCGCAGAGGCCGTGGGGTCTTCGCTGT GGTGCG
Alp-LHinge-R	TTTGCTCTGCGGCCGCAGAGGCCGATTGTGGTTTTGGTGT CTTGGG
Alp-FR3-overlap-F	TCCGTGAAGGGCCGATTC
Alp-FR3-overlap-R	GAATCGGCCCTTCACGGA
New left-F	GATCCCGCGAAATTAATACGACTCACTATAGGG
cnvKpolyA-R	TTTCCACGCCGCCCCCCGTCCT
qPCR VHH 1 Forward	CAAGGCCAAGAACACGGTGTATC
qPCR VHH 1 Reverse	TCGAGATCTTCCTCTCCACGTACTAC
qPCR VHH 2 Forward	CGAATGGCGGCACTATCACA
qPCR VHH 2 Reverse	CTCCAGCTGATAGCGGCTACAA
qPCR VHH 3 Forward	GCTCTAATTCGATGGCCTGGTT
qPCR VHH 3 Reverse	CCACATAGCCCGTGTTACCATTTC
BDA_qPCR (+)	CTACAAGCCACCATGGATAAC

BDA_qPCR (-)	GCTTGGGTCATCTTTTAGGC
GFPVHHqPCRFw	AACACCATCCTGGGCGATAG
GFPVHHqPCRRv	GTGTTTTTGGCGCGATCAC

Table 4. Amino Acid sequences of the candidate VHHs.

Fragment name	**Amino Acid sequence**
VHH1	AEVQLVESGGGLVQAGGSLRLSCAINDRTFSNYSMGWFR QAPGKEREFVAAITHNGSTNFPDSVKGRFTISVDKAKNTV YLQMNSLKPEDTAVYYCAVDHSFITVVRGEEDLEVWGQ GTLVTVSSAHHSEDPT
VHH2	AEVQLVESGGGSVQAGGSLRLSCSASGPEWRHYHMGWF RQPPGKEREFVAAISWSGGTTMYADSVKGRFTISRDNVK NTVYLQMNSLKPEDTAVYYCAAGDTVVALLDYRAYWG QGTQVTVSSEPKTPKPQS
VHH3	AEVQLVESGGDLVQPGGSLNLSCVADATIFGSNSMAWFR QYPGKQRDLLATVARNGNTGYVDSVKGRFTISRDDGQNI VYLQMNSLKPEDTALYTCNLKRYRMGFILDGDYWGQGT QVTVSSEPKTPKPQS

Table 5. Abbreviations

VHH	Camelid heavy-chain antibody VH
cDNA	Complementary DNA

PCR	Polymerase chain reaction
cD-iPCR	cDNA display mediated immuno-polymerase chain reaction
mRNA	Messenger RNA
ELISA	Enzyme-linked immunosorbent assay
CDR	complementarity determining region
cnvK	3-cyanovinylcarbazole nucleoside
qPCR	quantitative polymerase chain reaction
PAGE	Polyacrylamide gel electrophoresis
SDS	sodium dodecyl sulfate
TBE	Tris/Borate/EDTA
MES	2-(N-morpholino)ethanesulfonic acid
PBS	Phosphate-buffered saline
UV	Ultraviolet
FITC	Fluorescein isothiocyanate
SA beads	Streptavidin Magnetic Beads
Ni-NTA	nickel-charged affinity resin
DTT	Dithiothreitol
NGS	Next-generation Sequencing
BSA	Bovine serum albumin
HPR	horseradish peroxidase enzyme
Ct	Cycle threshold
DMSO	Dimethyl sulfoxide
GFP	Green Fluorescent Protein

BDA	B Domain protein A
IgG	Immunoglobulin G

Table 6. ELISA absorbance data (for Figure 2.11A)

VHH concentration µg/mL	Gliadin + VHH1	Gliadin + VHH2	Gliadin + VHH3	Gliadin + Anti-BSA VHH	BSA + Anti-BSA VHH
0	0.049	0.044	0.048	0.036	0.031
0.15	0.087	0.090	0.037	0.033	0.258
0.31	0.124	0.116	0.041	0.033	0.391
0.62	0.194	0.151	0.043	0.033	0.625
1.25	0.298	0.227	0.051	0.038	0.955
2.5	0.458	0.354	0.084	0.051	1.581
5	0.535	0.484	0.120	0.054	2.024
10	0.733	0.684	0.218	0.072	2.148

Table 7. Standard deviation data for Figure 3.5

Spiked Concentration (ng/mL)	VHH1		VHH2	
	Rice	Buffer	Rice	Buffer
0	0.175	0.116	0.032	0.045
0.05	0.202	0.067	0.112	1.259
0.5	0.087	0.282	0.342	0.195
5	0.627	0.050	0.813	0.227

Table 8. Primers used in the NGS analysis.

Primer name	**sequence（5’ to 3’）**
prRd1N4VHH-F	TCGTCGGCAGCGTCAGATGTGTATAAGAGACAGNNN NATGGCTGAGGTGCAGCTCGTG
prRd2N4VHH-R	GTCTCGTGGGCTCGGAGATGTGTATAAGAGACAGNN NNTGATGATGATGGCTACCACCTCCCG
prNexteraXTIndex1(N701)	CAAGCAGAAGACGGCATACGAGATTCGCCTTAGTCT CGTGGGCTCGG
prNexteraXTIndex1(N702)	CAAGCAGAAGACGGCATACGAGATCTAGTACGGTCT CGTGGGCTCGG
prNexteraXTIndex1(N703)	CAAGCAGAAGACGGCATACGAGATTTCTGCCTGTCT CGTGGGCTCGG
prNexteraXTIndex1(N704)	CAAGCAGAAGACGGCATACGAGATGCTCAGGAGTCT CGTGGGCTCGG
prNexteraXTIndex1(N705)	CAAGCAGAAGACGGCATACGAGATAGGAGTCCGTCT CGTGGGCTCGG
prNexteraXTIndex1(N706)	CAAGCAGAAGACGGCATACGAGATCATGCCTAGTCT CGTGGGCTCGG
prNexteraXTIndex1(N707)	CAAGCAGAAGACGGCATACGAGATGTAGAGAGGTCT CGTGGGCTCGG
prNexteraXTIndex1(N708)	CAAGCAGAAGACGGCATACGAGATCCTCTCTGGTCT CGTGGGCTCGG

prNexteraXTIndex1(N709)	CAAGCAGAAGACGGCATACGAGATAGCGTAGCGTCT CGTGGGCTCGG
prNexteraXTIndex2(N501)	AATGATACGGCGACCACCGAGATCTACACTAGATCGC TCGTCGGCAGCGTC

Materials and Reagents

Note: All reagents should be of molecular biology grade to avoid contamination of ribonuclease.

1. Polystyrene microtiter plate (MICROLON, 96 Well Single-Break Strip Plate, PS), Greiner Bio-One 705071.
2. PCR tubes (End point PCR tubes; TreffLab Laboratory Consumables, catalog number: 96.09852.9.01, qPCR strip tubes; SSIBio, catalog number: 3248-00).
3. DNA oligos can be obtained from custom DNA synthesis service. Eurofins Genomics (Ota-ku, Tokyo, Japan), Store at -20 °C.
4. PrimeSTAR HS DNA polymerase (Takara, catalog number: R010A). Store at -20 °C.
5. FavorPrep PCR Clean-Up Mini Kit (Favorgen). Store at room temperature.
6. RiboMAX™ Large-Scale RNA Production System T7 (Promega, catalog number: P1300). Store at -20 °C.
7. Wheat gliadin (RT) (Sigma, catalog number: G3375)
8. Dynabeads MyOne carboxylic acid beads (Invitrogen, catalog number: 65012).
9. RNA Clean-Up Kit (Favorgen, catalog number: FAPCK001), store at 4 °C.
10. Nuclease treated Rabbit Reticulocyte Lysate System, (Promega, catalog number: L4960). Amino acid mixtures for translation are included. Store at -80 °C.
11. RNasin® Ribonuclease Inhibitor (Promega; catalog number: N2111). Store at -20 °C.

12. Dynabeads MyOne streptavidin C1 (VERITAS; catalog number: DB65002). Store at 4 °C.
13. ReverTra Ace® (Toyobo, catalog number: TRT-101). 5× RT Buffer and 2.5 mM each dNTP mix are included. Store at -20 °C.
14. His Mag Sepharose Ni (GE Healthcare, catalog number: 2896390)
15. RNase T1 (1,000 U/L) (Thermo Fisher Scientific, catalog number: EN0541)
16. RNase H (Takara, catalog number: 2150A, 10 U) and 10× NE buffer 2 (NEB)
17. DL-Dithiothreitol ≥ 99.0% (RT) (Sigma, catalog number: 4381)
18. Quick-Load 100 bp DNA Ladder, (Biolabs: catalog number: N0467), NEB
19. SYBR Gold Nucleic Acid Gel Strain (Invitrogen, catalog number: S11494)
20. THUNDERBIRD SYBR qPCR Mix (Toyobo, catalog number: QPS-201)
21. 10x PBS (Phosphate-buffered saline -) (Wako, catalog number: 163-25265)
22. Skim milk (Wako, catalog number: 190-12865)
23. NaCl (Wako, catalog number: 191-01665)
24. Tris-HCl (Wako, catalog number: 208-14691)
25. KCl (Wako, catalog number: 163-03545)
26. $MgCl_2$ (Wako, catalog number: 136-03995)
27. EDTA (Invitrogen, catalog number: 15575-038)
28. Urea (Wako, catalog number: 217-01215)
29. Bromophenol Blue (BPB) (Wako, catalog number: 021-02911)
30. Xylene Cyanol (XC) (Wako, catalog number: 244-00461)
31. UltraPure DNase/RNase-Free Distilled Water (UPDW)
32. Ammonium persulfate (Wako, catalog number: 012-20503)
33. Acrylamide (Nacalai tesque, catalog number: 00807-05)

34. Tetramethylethylenediamine (TEMED) (Wako, catalog number: 205-06313)
35. Tween20 (Sigma-Aldrich, catalog number: P9416)
36. Sodium phosphate Dibasic (Wako, catalog number: 042-29445)
37. Imidazole (Wako, catalog number: 095-05392)
38. 40% (w/v) Acrylamide-Bis (Nacalai tesque, catalog number: 00857-55)
39. Hydrochloric acid (HCl) (Sigma-Aldrich, catalog number: 320331)
40. Tris-borate-EDTA (TBE) Buffer (10X) (Invitrogen, catalog number: B52)
41. Tris-EDTA (TE) buffer (Invitrogen, catalog number: AM9849)
42. N-hydroxysuccinimide (NHS) (Tokyo chemical industry, catalog number: B0249)
43. 1-ethyl-3-(3-dimethylaminopropyl) carbodiimide hydrochloride (EDC) (Tokyo chemical industry, catalog number: D1601)

Equipment

1. Thermal cycler (Biometra, Model: TRIO48)
2. Biomolecular imager (GE healthcare, Model: Typhoon FLA9500)
3. NanoDrop Spectrophotometer (Thermo Scientific, Model: 1000 V3.3)
4. NanoDrop Spectrophotometer (Thermo Scientific, Model: 3300 V2.7, FITC)
5. Heat block (ANATECH, Model: cool stat 5200)
6. UV Crosslinker (UVP, Model: CL-1000)
7. Vortex mixer (IWAKI, Model: TM 2000)
8. Magnetic separator (Invitrogen, Model: 12320D)
9. Thermo block rotator (NISSIN, Model: SNP 24B)
10. StepOne Real-Time PCR System, (Thermo Fisher Scientific, Model: 4376600)
11. High speed refrigerated microcentrifuge (KITMAN, Model: Tomy Tech MX-301)

12. Gel electrophoresis apparatus (PAGE/SDS-PAGE) (ATTA, Model: AE 6510)

13. Pipettes (Gilson Pipetman, Model P2- P1000)

Software

1. Quantity One 1-D Analysis Software (Bio-Rad, Version 4.6.6)
2. Primer Express (Thermo Fisher Scientific, Version 3.01)